



Natural Resources
Canada

Ressources naturelles
Canada

**GEOLOGICAL SURVEY OF CANADA
OPEN FILE 8579**

**Synthesis of near-bed currents and sediment mobility on the
Beaufort Shelf edge and upper slope, offshore Northwest
Territories**

M.Z. Li, E.L. King, A. Forest, H. Melling, and P.D. Osborne

2020



GEOLOGICAL SURVEY OF CANADA OPEN FILE 8579

Synthesis of near-bed currents and sediment mobility on the Beaufort Shelf edge and upper slope, offshore Northwest Territories

M.Z. Li¹, E.L. King¹, A. Forest², H. Melling³, and P.D. Osborne⁴

¹Geological Survey of Canada, 1 Challenger Drive, Dartmouth, Nova Scotia

²Amundsen Science, Université Laval, 1045 Avenue de la Médecine, Quebec, Quebec

³Institute of Ocean Sciences, Fisheries and Oceans Canada, 9860 West Saanich Road, Sidney, British Columbia

⁴Golder Associates Ltd., 500 - 4260 Still Creek Drive, Burnaby, British Columbia

2020

© Her Majesty the Queen in Right of Canada, as represented by the Minister of Natural Resources, 2020

Information contained in this publication or product may be reproduced, in part or in whole, and by any means, for personal or public non-commercial purposes, without charge or further permission, unless otherwise specified.

You are asked to:

- exercise due diligence in ensuring the accuracy of the materials reproduced;
- indicate the complete title of the materials reproduced, and the name of the author organization; and
- indicate that the reproduction is a copy of an official work that is published by Natural Resources Canada (NRCan) and that the reproduction has not been produced in affiliation with, or with the endorsement of, NRCan.

Commercial reproduction and distribution is prohibited except with written permission from NRCan. For more information, contact NRCan at nrcan.copyrightdroitdauteur.nrcan@canada.ca.

Permanent link: <https://doi.org/10.4095/326562>

This publication is available for free download through GEOSCAN (<https://geoscan.nrcan.gc.ca/>).

Recommended citation

Li, M.Z., King, E.L., Forest, A., Melling, H., and Osborne, P.D., 2020. Synthesis of near-bed currents and sediment mobility on the Beaufort Shelf edge and upper slope, offshore Northwest Territories; Geological Survey of Canada, Open File 8579, 58 p. <https://doi.org/10.4095/326562>

Publications in this series have not been edited; they are released as submitted by the author

Table of Contents

Executive Summary	1
1. Introduction.....	2
2. State of knowledge on dominant oceanographic and sediment transport processes.....	3
2.1 Water masses and circulation at the Beaufort shelf edge and upper slope.....	3
2.2 Sediment sources and transport processes on the shelf.....	4
2.3 Oceanographic and sediment transport processes on the shelf edge and upper slope	6
3. Magnitude and frequency of near-bed currents and sediment mobility.....	7
3.1 Data types and methods	7
3.1.1 Surficial geology.....	7
3.1.2 Current data.....	8
3.1.3 Estimates of bottom currents with Soulsby’s method.....	9
3.1.4 Erosion threshold and sediment erosion frequency estimation.....	14
3.1.5 Possible pre-conditions affecting erosion threshold	17
3.2 Near-bed currents and sediment mobility at western Beaufort Shelf-Mackenzie Trough (WBS-MT) area.....	17
3.3 Near-bed currents and sediment mobility at western Central Beaufort Shelf (WCBS) area	22
3.4 Near-bed currents and sediment mobility at eastern Central Beaufort Shelf (ECBS) area.....	33
3.5 Near-bed currents and sediment mobility on the eastern Beaufort Shelf (EBS).....	41
3.6 Discussion of near-bed currents and sediment mobility analyses.....	44
3.6.1 Overall characteristics of current intensity and sediment erosion frequency.....	44
3.6.2 Seasonality of bottom currents and isobaths control of current direction.....	45
3.6.3 Inter-annual variabilities	46
4. Oceanographic processes and distribution of the erosion/non-deposition zone	46
4.1 Characteristics and distribution of the erosion/non-depositional zone	46
4.2 Correlation of erosion/non-depositional zones with oceanographic processes.....	47
5. Summary.....	52
Acknowledgement	54
References.....	55

Executive Summary

Limited wind-driven current modelling and moored current measurements suggest the presence of strong currents associated with the amplified Beaufort Shelf-break Jet (BSJ) on the Beaufort shelf edge and upper slope. Zones of erosion and non-deposition have also been mapped along the shelf break. However, knowledge of near-bed current intensity and erosion and transport of sediments on the Beaufort shelf break and upper slope is lacking. This report addresses the lack of near-bed current data and the gap in our understanding of the spatial distribution of bottom currents and sediment mobility on the Beaufort shelf edge and upper slope through the compilation and analysis of existing moored current data. The spatial patterns of bottom currents and sediment mobility are compared with the mapped distribution of the erosion and non-deposition zones for insights of the correlation between modern oceanographic processes and the distribution of the erosion and non-deposition zones on the Beaufort shelf break and upper slope.

Mooring water-column and near-bed current data have been compiled from 11 sites that occur in water depths of 75–660 m and span the entire Beaufort shelf break and upper slope environments. The measured and extrapolated near-bed current data, largely at 6–10 m above bottom, were analyzed and compared with the threshold for sediment erosion to derive a regional framework of near-bed currents and sediment mobility on the Beaufort Shelf break and upper slope. Events with maximum bottom currents of 60-80 cm/s periodically occur and maximum sediment erosion frequency can reach 17% and 7% of the time on the Beaufort shelf break and upper slope respectively. These estimates suggest that currents and sediment mobility on the Beaufort shelf break and upper slope are greater than the mid- and outer shelf. The direction of peak currents is roughly parallel to the local isobaths, predominantly to the NE and the ENE on the central Beaufort shelf break. The bottom currents and inferred sediment mobility also show strong seasonal and inter-annual variabilities.

Estimated near-bottom currents and sediment erosion frequency along cross-slope transects demonstrate that currents and sediment erosion are the strongest along the shelf break and decrease both seaward on the upper slope and landward on the outer shelf. The width of the impact zone of the amplified Beaufort Shelf-break Jet currents is 20–25 km. Intensity of currents and sediment erosion also decreases from the west to the east. These observations are in qualitative agreement with the width and along-slope trend of the mapped erosion and non-deposition zone, suggesting that the presence and amplification of the BSJ are responsible for this seabed phenomenon.

1. Introduction

Limited wind-driven current modelling (Williams and Carmack, 2010) and moored current measurements (e.g. Forest et al., 2007, 2008) suggest that strong currents can occur on the Beaufort shelf edge and upper slope. Oil and gas industry expressed concerns on how current strength and seabed instability may constrain their exploration and production operations (Steve Blasco, personal communication, 2013). A shelf-edge zone of erosion has long been recognized (Blasco et al. 2013, Woodworth-Lynas et al. 2016). Detailed mapping (King et al., 2016, 2017) has further demonstrated the occurrence of the erosional zone as well as a non-depositional zone that extend ~300 km along the shelf break and upper slope with a trend of decreasing widths from the west to the east (Fig. 1). Several studies have analyzed site-specific data of currents, sediment concentration, and particulate mass flux to suggest that the strong currents may be responsible for the erosion of sediments on the Beaufort shelf edge and upper slope (e.g. Forest et al., 2015; 2016). Based on limited bottom current data and the coincidence between the spatial patterns of modelled shelf-edge currents and the distribution of the mapped erosion and non-deposition zones, King et al. (2016, 2017) proposed a causal relationship between the erosion and non-deposition zones and the amplified shelf-break currents. To date there has been no systematic study of the spatial distribution of bottom currents, sediment mobility and transport on the outer shelf and slope in the Beaufort Sea. Furthermore, most mooring observations to date have been limited to current measurements at heights greater than a few tens to several hundred meters above the seabed. Knowledge of near-bed (0 to a few meters above seabed) current intensity and erosion and transport of sediments on the Beaufort shelf break and upper slope is lacking.

The purpose of this report is to begin addressing the lack of near-bed current data and the gap in understanding the spatial distribution of bottom currents and sediment mobility on the Beaufort shelf edge and upper slope. Existing moored current data have been compiled and evaluated for selected geographic areas along the Beaufort Shelf. Water column currents at some of the selected sites have been extrapolated to near-bed currents. The existing measured and extrapolated near-bed currents have been analyzed and compared with the threshold for sediment erosion to systematically characterize the spatial distribution of near-bed currents and sediment mobility along the Beaufort Shelf break and upper slope. The spatial patterns of bottom currents and sediment mobility are then compared with the mapped distribution of the erosion and non-deposition zones for insights of how the mapped erosion and non-deposition zones match with modern oceanographic processes on the Beaufort shelf break and upper slope. Following the Introduction, Section 2 provides a review of the state of the knowledge on dominant oceanographic and sediment transport processes. The study methods and the analysis results of the magnitude and frequency of near-bed currents and sediment mobility for various geographic areas are presented in Section 3. The characteristics and distribution of the erosion and non-deposition zones on the Beaufort shelf edge are described and its correlation with oceanographic

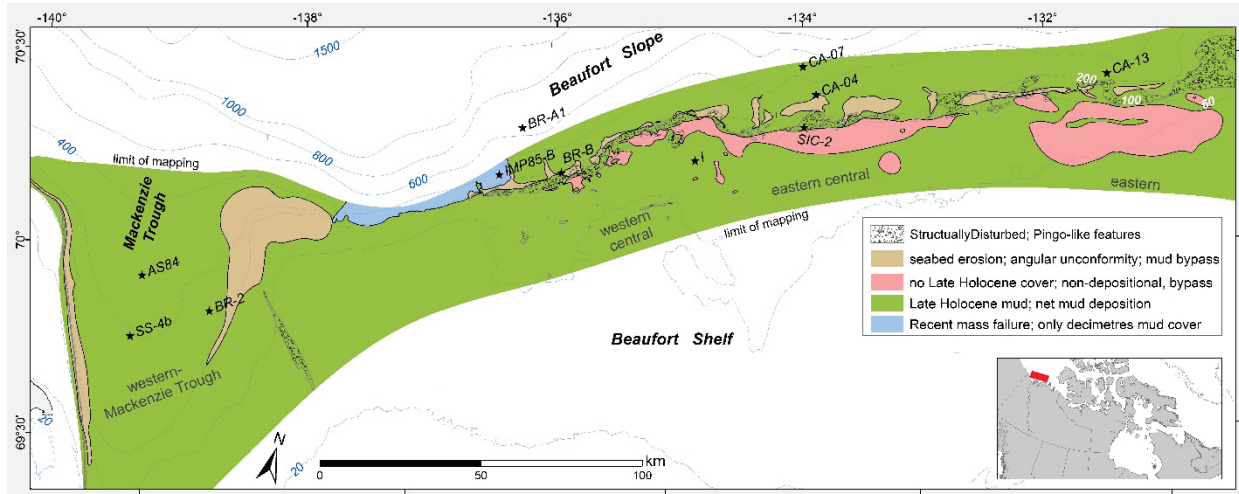


Figure 1 Names and locations of the current mooring sites (stars) on the Beaufort outer shelf and upper slope superposed on the mapped erosion and non-deposition zones (modified from King et al. 2017) consisting of various geological units that are shown in the legend box and described in text. Relevant information of the mooring sites is given in Table 1.

processes is explored in Section 4. The last section provides a summary of key findings of this synthesis study.

2. State of knowledge on dominant oceanographic and sediment transport processes

A range of topographic regions will be referred to through out this report. Reviews of literature and the gradient of depth change, as a function of offshore distance, have been used to define shelf edge (break) as 80 – 100 m water depths, upper slope from 100 – 300 m water depths, middle slope from 300 – 600 m water depths and the base of slope is at 2200 m water depth. The definitions of topographic regions on the shelf follow Hill et al. (1991). The inner shelf is defined in water depths <20 m, middle shelf from 20 – 60 m water depths and outer shelf from 60 – 80 m water depth.

2.1 Water masses and circulation at the Beaufort shelf edge and upper slope

Waters of Pacific Ocean origin intrude the western Arctic Ocean through the Chukchi Shelf and integrate with the Atlantic Waters that enter the Arctic Ocean through Fram Strait and flow counter clockwise along the margin of the Arctic Ocean, to form three vertical layers in the offshore of the Beaufort Sea (Coachman and Barnes, 1961; Carmack and MacDonald, 2002; Forest et al., 2008). The relatively fresh Polar-Mixed surface layer (PML; <50 m depth with

salinity $S < 32\text{‰}$) overlies the Pacific-derived halocline (PH, 50–200 m depth with $32 < S < 34$) overlying the deep and more saline Atlantic Waters (AW; > 200 m depth with $S > 34.5$).

Tidal currents in the Beaufort Sea are semi-diurnal but very weak, of the order of 2–3 cm/s (Giovando and Herlinveaux, 1981). Hydrodynamics on the Beaufort shelf break and slope are thus dominated by large-scale ocean circulation systems and regional meteorological-oceanographic interactions. The surface ocean circulation over the shelf break and slope are dominated by westward currents in the southern branch of the anticyclonic Beaufort Gyre (Giovando and Herlinveaux, 1981; Carmack and MacDonald, 2002; Lukovich and Barber, 2006). The water reverses to cyclonic (flowing eastward) below the surface layer (Carmack and MacDonald, 2002). The subsurface flow thus moves Pacific-origin waters eastward along the continental slope within the Beaufort Shelf-break Jet (BSJ), formerly known as the Beaufort Undercurrent (Aagaard, 1984). The BSJ is a narrow (20 km width) bathymetrically steered eastward countercurrent following the shelf slope from around the 50 m isobath to at least the base of the continental slope (Pickart, 2004). Recent studies have refined our understanding of this circulation and suggest that the BSJ is more intense from about 50 to 200 m depth, resulting in a narrow current (10–15 km width) trapped on the upper continental slope (Pickart, 2004; Pickart et al., 2005; Forest et al., 2008; Nikolopoulos et al., 2009).

The Beaufort Gyre and BSJ are both highly sensitive to wind forcing (O'Brien et al., 2011). O'Brien et al. (2006) suggest that the currents within the BSJ are subject to frequent reversals to the west, which are normally associated with upwelling onto the outer shelf (Aagaard, 1984). On a regional scale, circulation currents and the amplification of these currents are important on the outer shelf and continental slope, while storm waves and wind-forced currents are more dominant on the mid- and outer-shelf areas (IORVL, 2013). Currents are expected to be the strongest at the shelf edge, while the circulation on the shelf is highly variable (Melling, 1993; Kulikov et al., 1998; O'Brien et al., 2006).

2.2 Sediment sources and transport processes on the shelf

Sediments are predominantly supplied to the Beaufort Sea by the Mackenzie River delivering $\sim 125 \text{ Mt yr}^{-1}$ of mainly fine grained sediment from which a substantial fraction (40% or 50 Mt) is deposited in the delta, leaving 50 to 70% ($\sim 75 \text{ Mt}$) as sediments delivered to the inner shelf (Hill et al., 1991; Macdonald et al., 1998; Carson et al., 1998; Osborne and Forest, 2016). Minor contributions of sediment are derived from other rivers (1.5 Mt yr^{-1}) and from the erosion of coastal bluffs (5.6 Mt yr^{-1}). The uppermost layer of the surficial sediments on the floor of the Beaufort Sea comprises silty clay and fine sands ranging in thickness from a few centimeters on the eastern shelf to several meters in the west (Blasco et al., 2013). The sediments discharged from the river move across the shelf to the shelf edge and upper slope via cycles of deposition, resuspension and transport that are mainly controlled by the extent of the open water, the

dispersal and transport by the turbid Mackenzie River plume during freshet, and the intense resuspension and transport by strong waves and wind-driven currents associated with storms (Hill et al., 1991; Macdonald and Yu, 2005; O'Brien et al. 2006; O'Brien et al. 2011). Through integrating published sediment fluxes and recent mooring and ship-based measurement data, Osbourne and Forest (2016) developed a model of sediment pathways for the Canadian Beaufort Sea using the reverse analysis methodology. The model estimates that the initial annual delivery of sediments from the delta to inner shelf is ~79 Mt. Of the 79 Mt supply, ~63 Mt (80% of the annual delivery) is deposited on the shelf and ~15.2 Mt (20% of the annual delivery) are exported beyond the shelf edge to the slope. Approximately 7 Mt of the 15.2 Mt that reached the slope is deposited over the slope and ultimately ~8 Mt (10% of the initial annual delivery from the delta) is exported to the deep basin.

The transport of suspended sediments within the Mackenzie River plume is strongly influenced by ice cover, winds, and circulation currents (O'Brien et al. 2006). Northwesterly winds drive the plume eastward along the Tuktoyaktuk Peninsula (Giovando and Herlinveaux, 1981), whereas southeasterly winds push the plume to the west out over the Mackenzie Trough (MacNeill and Garrett, 1975). Under ice-free conditions, the plume can extend well into the Canada Basin (Macdonald et al., 1998). During the open-water season, the Beaufort Sea shelf is mainly influenced by wind-driven waves and currents (Hill et al., 1991; Macdonald and Yu, 2005; O'Brien et al., 2011). Storm winds sometimes reach 80 km/h during this period of large fetch and cause high waves and wind-driven currents that result in widespread sediment resuspension and transport on the shoreface and inner shelf (Hill and Nadeau, 1989; Hill et al., 1991). Héquette et al. (2001) indicated that high wave orbital velocities (up to 50 cm/s) during northwesterly storms induce significant sediment remobilization on the shoreface (3.4 m water depth) and strong and sustained seaward directed near-bottom currents cause offshore dispersal of shoreface sediments that may be transported to depths from which fair weather waves may not be capable of returning the material onshore. Over the mid- and outer shelf, Hill et al. (1991) suggested that wave motions influence bottom sediment transport less than 1% of the time and that near-bottom currents were weakly coupled to surface winds to cause occasional sediment resuspension during storms. Recent measurements on the outer shelf, however, suggest that the near-bottom currents are actually well coupled with wind dynamics and the advection of fine particles to the shelf edge should be expected during downwelling-favorable wind conditions (Osborne and Forest, 2016). In the 1:1 year storm of late August 1987, peak significant wave height H_s was > 3 m and peak wave period T_p was 8 s. O'Brien et al. (2006) estimated that the near-bed wave orbital velocity would exceed 25 cm/s and cause sediment resuspension to at least the depth of 50 m. Based on the extremal analysis using 43 year (1970 – 2012) wave hindcast predictions for the Beaufort Sea (Swail et al., 2007), the peak significant wave height H_s would reach 6.1 m and the peak wave period T_p will be 10.6 s on the mid-shelf during a 1:50 year storm. It can be expected that significant sediment resuspension and transport would occur on the Beaufort Shelf during extreme storms.

Once sediments are resuspended, they are transported across and along the shelf by wind-driven and downwelling currents through the development of both the bottom and intermediate Nepheloid layers (BNL and INL, respectively; O'Brien et al. 2006, 2011; Forest et al. 2007, 2008; Osborne and Forest, 2016). Several intense events with winds exceeding 10 m/s predominantly from the northwest in August and September of 1987 produced persistent offshore (downwelling) bottom currents of 25 – 50 cm/s in the nearshore that typically continued for 1 – 2 days (Hequette et al., 2001). Based on transmissometer and sequential sediment trap data collected over this period, O'Brien et al. (2006) suggested that the strong waves and downwelling currents during storms with northwesterly winds cause intense sediment resuspension and that shelf sediments are episodically transported to the edge of the Beaufort Shelf in the BNL and INL. Transmissivity and density data collected in October 2003 along an outer shelf–slope transect have been used by Forest et al. (2007) to further demonstrate that the resuspension of sediments on the shelf caused the development of a well-defined BNL over the shelf and that the water of the BNL extended horizontally over the slope along an isopycnal, forming a mid-depth INL over the slope. They suggest that coastal wind storms likely combined with thermohaline convection following rapid ice growth to resuspend shelf sediments and mix the BNL in October–November 2003. Nevertheless, the conditions required to set the Nepheloid Layers in motion were not well understood. More process-oriented studies targeting the shelf bottom boundary layer and water column structures are needed to resolve the mechanisms underlying the formation and motion of the BNL and INL at various time scales and their interaction with the BSJ on the upper slope.

2.3 Oceanographic and sediment transport processes on the shelf edge and upper slope

Analyses and interpretation of current and sediment trap data from oceanographic moorings presented in several studies provide preliminary evidence that the presence and surges of the BSJ, the generation and meandering of eddies associated with the BSJ, and the generation and descending of cold dense winter water are the dominant processes that cause erosion and transport of sediments on the Beaufort shelf edge and upper slope (Forest et al. 2007, 2008, 2015; O'Brien et al. 2011).

Forest et al. (2007, 2008) reported episodic strong currents in the water column and associated high particle fluxes over the upper slope (at 200 m over the 300 m isobath) in the winters of 2004, 2005, and 2006. Each winter, an abrupt and brief (<8 days) amplification of the subsurface eastward circulation of the BSJ was recorded when sea ice covered most of the western Arctic Ocean. Compared to a mean background speed of ~9 cm/s, the highest daily mean speeds recorded during these events reached 67, 94 and 62 cm/s, respectively in 2004, 2005 and 2006. The downward particle flux estimated with the sediment traps reached their annual peak values at approximately the same time as the abrupt current surges were recorded. Based on the

temporal correlation between the enhanced currents and the high particle fluxes and analyses of ice coverage, temperature, wind and current data associated with the recorded peaks of downward particle fluxes, Forest et al. (2007, 2008) proposed that these events were attributed to local resuspension and subsequent dispersal of bottom sediments over the upper slope due to the abrupt current pulses of the intensified BSJ and strong rotary currents of eddies formed by baroclinic instability of the BSJ (O'Brien et al., 2011). Thermohaline convection associated with rapid ice formation as well as wind forcing of storms could cause the amplification of the BSJ. Forest et al. (2015) have used additional mooring data from September 2009 to August 2012 over the Beaufort slope to further illustrate the potential processes that drive the lateral transport of particulate matter off the shelf. Particle fluxes data have been considered along with synchronous current time-series, water column properties and meteorological data to further suggest that thermohaline convection and downwelling-favorable storm winds act as the main mechanisms underlying the resuspension and offshore transport processes. Their combination drives mesoscale eddy formation, downwelling flows and current surges that are characterized by moderate to high current speeds (20–80 cm/s) in the water-column and sufficient to mobilize sediments. It should be noted that most mooring studies provide daily averaged currents measured 10s to 100s meters above the seabed and that the maximum speeds of such currents measured in the water column are 90 – 120 cm/s and are predominantly to the northeast (Forest et al., 2008; Dmitrenko et al., 2016). Near-bottom current and sediment transport measurements are rare to non-existent on the Beaufort shelf break and upper slope. Only a recent study by Forest et al. (2016) presented strong currents up to ~40 cm/s within the lowermost 10 m bottom layer at two shelf break locations and found that sudden peaks in suspended sediments corresponded closely with the current surges implying the local erosion of surficial sediments at these shelf break sites. Magnitude and spatial patterns of the BSJ and the amplification impact on the BSJ by various oceanographic processes remain poorly understood.

3. Magnitude and frequency of near-bed currents and sediment mobility

3.1 Data types and methods

3.1.1 Surficial geology

The seabed geology maps for the entire Beaufort shelf in Figure 1 and for selected geographic areas depict zones of erosion (brown) and non-deposition (red). They are derived from analysis of a network of 3.5 kHz sub-bottom profiler data, primarily collected on the R/V CCGS Amundsen through the ArcticNet consortium of university, government and industry collaborations since 2006. The sub-bottom profiler data were amassed from tracks across 14 cruises from which over 35,000 km covering the map area were interpreted. Chronology is from C-14 dates on shells and foraminifera from about 25 shelf-break and upper slope-situated sediment core sites, including over 70 dates. Many dates are reported in Woodworth-Lynas et al.

(2016) or reside in the GSC Expedition Database. The correlation of these dates with the sub-bottom profiler records across the region into a chronology framework is briefly summarized in King et al. (2017).

The map in King et al. (2017) has been updated here to include more detail and larger geographic scope (Fig. 1). The criteria for mapping the erosion zone was an angular unconformity in the Holocene age sediments. The smooth nature of the erosion and non-deposition zones largely precludes its recognition from multibeam bathymetric shaded relief images. The non-depositional zone is recognized by a generally gradual thinning from shelf to shelf-break, typically from 10 m thick, to under 0.5 m, the approximate resolution limit for its recognition. Recognition of the erosion and non-deposition zones is strongly compromised where it has been structurally disturbed by a combination of localized diapiric and subsidence processes associated with thousands of mounds and moats, so-called “pingo-like features” (PLFs) and related ridges and trenches. These have tilted and disturbed strata, often to the point of lost seismic reflector coherence on stratal horizons such that the mapping criteria are not met. These disturbed zones are shown by the hatch pattern on the maps. In general it is likely that these disturbed zones also encompass both erosion and non-deposition, but probably with very local variation. Lee-side deposition complementing stoss side erosional moats on some PLFs is an example of the occurrence of both erosion and non-deposition in the disturbed zones (King et al. 2017). Fig. 1 shows that non-deposition zones were only mapped landward of the erosion zone. Given the fact that the BSJ currents are strongest over the shelf break and decrease both landward and seaward, the non-deposition zone should exist both landward and seaward of the erosion zone and the mapped non-deposition zone should adjoin the erosion zone. However, the mapping constraints noted above, together with the structural disturbance, present a challenge in mapping to this detail.

The chronology framework demonstrated a temporal evolution in the erosional zone from net deposition to net erosion, which occurred in the early to mid Holocene (King et al. 2017), as the modern oceanographic regime adjusted to post-glacial eustatic sea-level rise.

3.1.2 Current data

Deployments of instrumented landers have been undertaken recently by the Geological Survey of Canada-Atlantic (GSCA) (Li et al., 2019) and the data from these will provide information of bottom currents and seabed responses, but the temporal and spatial coverage of the lander observation is limited, necessitating the use of measurements from existing current moorings. Existing mooring and near-bed current data have been compiled from various sources including ArcticNet and the Institute of Ocean Sciences of Fisheries and Oceans Canada (DFO). Existing data from 11 sites spanning the entire upper slope of the Beaufort Sea were eventually selected and analyzed in this synthesis study. These sites were selected based on the criteria of being

located close to the shelf edge and upper slope, availability of both near-bottom and water column current measurements, proximity to other mooring sites to form cross-slope transects, and the along-shelf locality that facilitates the current and sediment erosion evaluation along the entire Beaufort shelf break and upper slope. Figure 1 shows the names and locations of these sites. The detailed relevant information for each site is given in Table 1. Sites have been grouped into four geographic areas, from west to east, as follows: western Beaufort Shelf-Mackenzie Trough (WBS-MT) area, western central Beaufort Shelf (WCBS) area, eastern central Beaufort Shelf (ECBS) area and eastern Beaufort Shelf (EBS) area. The summary of current data in Table 1 indicates that the selected mooring data were collected from 1984 to 2013 and encompass outer shelf to continental slope settings in water depths of 75 – 660 m. Currents were measured near the bottom for six sites and current data for other sites were measured at a few tens to hundreds of meters above bottom (mab).

The shelf break or edge is the transition zone from the continental shelf to the slope. Although it is defined as 80 – 100 m water depths in this report, various depth ranges have been cited in the literature. Woodworth-Lynas et al. (2014) describes the shelf-to-slope transition was between ~100 m and 160 m water depths on the western Beaufort shelf. Although Forest et al. (2016) defines the shelf break as 80 – 100 m depths, they designate near shelf break as in 50 - 200 m depth and describe mooring sites in ~150 m water depth as near-shelf break setting. Our examination of detailed bathymetry contours also shows that the shelf to slope transition at some locations on the western central Beaufort shelf (~137° W and 70° 20' N) is best defined as from 80 - 250 m. Several selected sites of moored current data in Table 1 are in 110 – 160 m water depths and have been classified as near the shelf break, although they truly are on the upper slope.

3.1.3 Estimates of bottom currents with Soulsby's method

Current magnitudes typically decrease substantially above the seabed within the bottom boundary layer (BBL) due to bottom friction. Measured or modelled currents close to the seabed are required for adequate assessment of near-bed currents and sediment mobility on the Beaufort shelf edge and upper slope. The empirical method of Soulsby (1997) was applied to extrapolate current speed measured in the water column to near-bed values. For a variety of seabed types, the current profile can be approximated by an empirical power law that relates near-bed speed U_z at height z to depth-averaged speed U :

$$U_z = (z/0.32h)^{1/7}U \quad \text{for } 0 < z < 0.5h \quad (1)$$

$$U_z = 1.07U \quad \text{for } 0.5h < z < h \quad (2)$$

where h is the water depth. For the more typical cases in the marine environments, currents are often measured in the water column at significant heights above the bottom and depth-averaged

Table 1 Names and other relevant information of mooring sites used in this study.						
Site	Lat	Long	Water Depth (m)	Geomorphological settings and Geographic area	Data duration	Instruments, instrument depths and current data collected
Western Beaufort Shelf and Mackenzie Trough (WBS-MT)						
BR-2	69.9913	-137.9608	154	shelf break, east of Mackenzie Trough	2011 - 2013	Down-looking ADCP at 141 m depth in 2011 and at 137 m depth in 2012; Current profile data averaged over 80 sec every 1.5 hours for the bottom 10 m (2011) and averaged over 15 sec hourly for the bottom 13 m (2012) above bottom (mab).
SS4b	69.8500	-138.4930	200	upper slope of central Mackenzie Trough	1987/8 – 1988/3	RCM4 current meter at 150 m depth; hourly averaged current data at 50 mab
AS84	70.0200	-138.5750	280	upper slope of central Mackenzie Trough	1984/3 - 1985/8	RCM4 current meter at 274 m depth; hourly averaged current data at 6 mab
Western Central Beaufort Shelf (WCBS)						
I	70.8145	-134.5454	75	outer shelf, western central Beaufort Shelf	2009/7 - 2010/8 2010/8 - 2011/8	2009-10: ADCP at 70 m depth; continuous 15-min average data at 26 mab; 2010-11: ADCP at 60 m depth; continuous 15-min average data at 31 mab;
BR-B	70.6716	-135.5862	156	near shelf break, western central Beaufort Shelf	2009 - 2013	2009-11: ADCP at 140 m depth (2009-10) and at 124 m depth (2010-11), continuous 20 min average data at 35 mab (2009) and 25 mab (2010); 2011-12: down-looking ADCP at 142 m depth, current profiles averaged for 360 s in 2 hour intervals for the bottom 13 m 2012-13: down-looking ADCP at 140 m depth, current profiles averaged for 280 s in 1 hour intervals for the bottom 13 m
IMP85B	70.6133	-136.0750	302	upper slope, western central Beaufort Shelf	1985/4 - 1986/4	RCM4 current meter at 291 m depth; hourly averaged current data at 11 mab
BR-A1	70.7568	-136.0133	661	middle slope, western central Beaufort Shelf	2009 - 2013	2009-11: DVS750 current meters at ~671 m depth in ~684 m water depth, continuous 20-min average current data at 14-16 mab; 2011-13: Aquadopp Deepwater current meters at ~647 m depth in ~660 m water depth, current data averaged over 2 min hourly for 2011 and averaged over 4 min every half hour for 2012 at 13 mab;
Eastern Central Beaufort Shelf (ECBS)						
SIC2	70.9890	-133.7439	111	near shelf break, eastern central Beaufort Shelf	2010 - 2013	Up-looking ADCP at 107 m depth; continuous 40-min average current data at ~8 mab
CA04	71.0860	-133.7232	300	upper slope, eastern central Beaufort Shelf	2003 - 2006	RCM11 current meters at ~200 m depth; half-hourly (2003, 2005) or hourly (2004) averaged current data at ~100 mab

CA07	71.1498	-133.8980	500	middle slope, eastern central Beaufort Shelf	2003/10 - 2004/9 2004/9 - 2005/6	RCM11 current meters at ~387 m depth; half-hourly (2003) and hourly (2004) averaged current data at ~113 mab
Eastern Beaufort Shelf (EBS)						
CA13	71.3559	-131.3637	300	upper slope, eastern Beaufort Sea shelf	2003/10/9 - 2005/9/4	2003/10/9-2005/2/10: RCM11 current meter at 217 m depth, half-hourly averaged current data at 83 mab; 2003/10/9-2005/9/4: ADCP at 119 m depth, current data averaged for 12 min every 45 min at 192 mab;

current speed data are not available. The reversed equations (1) and (2) then can be used to compute the depth-averaged speed U from the measured water-column speed U_z :

$$U = U_z/(z/0.32h)^{1/7} \quad \text{for } 0 < z < 0.5h \quad (3)$$

$$U = U_z/1.07 \quad \text{for } 0.5h < z < h \quad (4)$$

The computed depth-averaged speed U could then be used in equations (1) and (2) to derive the near-bed speed at a small distance above the seabed. Comparison of measured and calculated normalized U_z/U over a wide variety of field measurements of various water depths, current speed, stratification conditions, flat or bedformed seabeds showed that the Soulsby method is applicable to the entire water column including the bottom boundary layer region and the errors in the predicted U_z/U are $\sim 10\%$ (Soulsby, 1997).

Measured bottom and water column currents were available for 2011-12 at BR-B site (Fig. 1 and Table 1). In order to evaluate the applicability of the Soulsby method over the Beaufort shelf edge/upper slope, the vertical profile data were used to derive the measured depth-averaged current speed U which was then used to calculate the predicted bottom current speed U_{11} at 11 mab. The ratios of predicted $U_{11_predicted}$ vs measured U_{11_obs} give a mean of 1.16 (with a standard deviation of 0.89). The scatter plot of $U_{11_predicted}$ vs U_{11_obs} is shown in Fig. 3-1a. The mean ratio and the scatter plot thus seem to support the application of the Soulsby method, albeit some significant scatters. The scatters and hence uncertainty partially can be attributed to the effect of surface Ekman layer, presence and vertical extent of the bottom logarithmic layer, spatial variations of density and stratification, and the presence of various oceanographic processes such as surges of the BSJ currents, cascading cold dense waters, up- and down-welling currents by storms, and the formation and migration of eddies. The calibration presented in Soulsby (1997) used the measured current speed normalized by the depth-averaged speed both of which were likely averaged over some time durations. The scatters shown in Fig. 3-1a could also partially due to that the predicted and measured bottom current speeds are directly compared and that the bottom current data were 360 s averages with 2 hour intervals. If the measured depth-averaged speed U and U_{11} were averaged over the deployment duration (~ 11 months), the observed ratio U_{11}/U was 0.9 and the predicted ratio was 0.81. The difference now is $\sim 11\%$ which is similar to the calibration errors presented in Soulsby (1997). To evaluate the applicability of Eq. (3) and (4), the measured current speeds at 46 mab, U_{46} , were used to calculate the predicted depth-averaged current speed $U_predicted$ from Eq. (3) and (4). The ratios of the predicted and observed depth-averaged current speeds, $U_predicted/U_observed$, have a mean value of 1.07. The scatter plot of $U_predicted$ versus $U_observed$ in Fig. 3-1b shows fair positive correlation (correlation coefficient 0.87) with moderate scatters. The mean ratio of $U_predicted/U_observed$ and their fair correlation suggest the application of Eq. (3) and (4) is adequate.

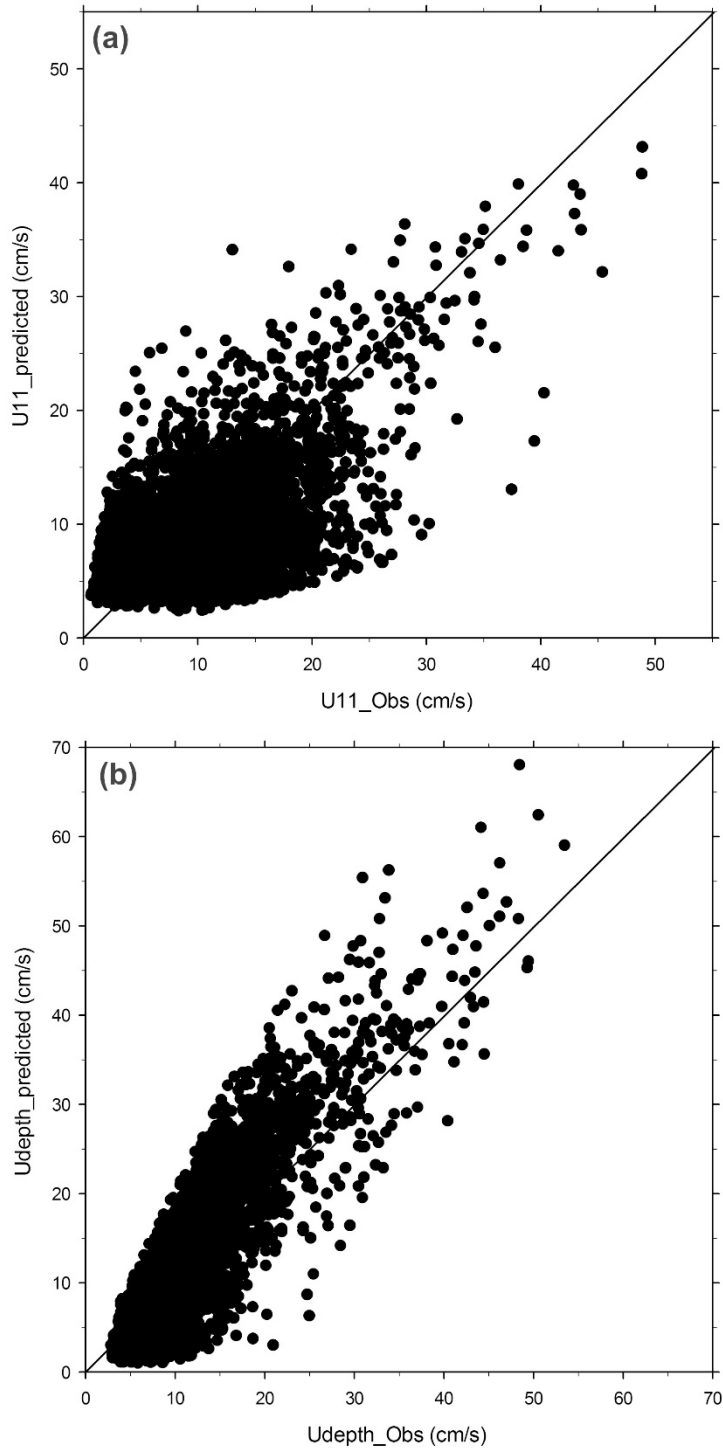


Figure 3-1 Scatter plots of (a) measured near-bottom current speed at 11 mab, $U11_{obs}$, versus that predicted by the Soulsby method, $U11_{predicted}$, and (b) measured depth-averaged current speed $Udepth_{obs}$ vs. that predicted by the Soulsby method, $Udepth_{predicted}$. Current data of 2011-12 at BR-B were used.

3.1.4 Erosion threshold and sediment erosion frequency estimation

Once the near-bed current speeds are computed, they can be compared with the threshold current speed at 1 m above the bottom, U_{100cr} , to estimate the frequency of sediment erosion. As sediments in the Beaufort Sea are dominantly fine grained (Hill et al., 1991; Blasco et al., 2013), sediments will go directly into suspension, by-passing the bedload transport mode once the currents exceed the threshold speed. Field data on the threshold for sediment transport on the Beaufort Shelf are lacking. Based on the laboratory measurements in a portable erosion chamber with a vertical oscillating grid, Walker et al. (2008) determined the threshold shear velocity u_{*cr} for several cores from the mid-shelf and upper slope of the Beaufort Sea. The threshold shear velocity is 1.05–1.30 cm/s for upper, less consolidated sediments and 1.3–1.7 cm/s for the lower, more consolidated sediments. O'Brien et al. (2011) estimated the range of critical current speed at 1 m above bottom, U_{100cr} , based on the quadratic-law and respective drag coefficients for mud and sandy mud. Given the winnowing effect from the intermittent erosion process and the small percentage of sand in the sediments on the Beaufort outer shelf and upper slope (Fig. 2 of Walker et al., 2008; Table 2 below), the surficial sediments on the Beaufort outer shelf and upper slope can be reasonably assumed to be sandy mud and the drag coefficient C_{100} would be 0.003 according to Dyer (1986) and Soulsby (1983). From the quadratic-law relating bed shear stress τ to near-bed current U_{100}

$$\tau = \rho u_{*cr}^2 = \rho C_{100} U_{100cr}^2 \quad (5)$$

the threshold shear velocity values of 1.05–1.3 cm/s for the less-consolidated upper layer will give the range of U_{100cr} from 19 – 24 cm/s. With u_{*cr} values of 1.3 – 1.7 cm/s for the more consolidated lower layer, the range of U_{100cr} will be 24 – 31 cm/s. The threshold $U_{100cr} = 19$ cm/s for the less consolidated upper layer is assumed in this study to achieve maximum estimates of erosion potential of the surficial sediments. The measured as well as extrapolated near-bed current speed based on equations (1) – (4) was compared to this threshold speed to estimate the cumulative time that sediment erosion occurred. The latter was then divided by the total measurement duration to derive the time percentage of sediment erosion or sediment erosion frequency. Currents were measured at 6 to 16 mab for majority of the sites for which near-bottom current data were available (Table 1). Ideally these near-bottom current data should be used in the logarithmic profile theory to further calculate the current speed at 1 mab, U_{100} which should then be compared with U_{100cr} to determine threshold exceedance. The application of the log profile theory, however, would require information of the bottom roughness which is unknown and depends on the sediment grain size and geometrics of bedforms. The estimate of bottom roughness as well as the presence and the vertical extent of the log velocity profiles would introduce further errors in the calculation of U_{100} . For these reasons, the bottom currents measured at 6-16 m heights were directly used in the comparison with U_{100cr} to determine the

exceedance of erosion threshold in this report. This approach will cause slight over-estimation of the frequency of sediment erosion in this study.

Texture and grain size information of existing grab and core samples on the Beaufort outer shelf and upper slope in the GSC Expedition Database has been accessed for the sediment types and mean grain size for the selected mooring sites and hence to evaluate the adequacy of the choice of the threshold criterion. For each of the selected current data sites, near-by grain size data were evaluated based on the integrated information of proximity to the current data site, water depth, and continuity of surficial geology between mooring and sample sites to select the most representative sample stations. The essential information of the selected grain size data for each of the current data sites is listed in Table 2. For current data sites for which the grain size data show significant variations or near-by grain size data are not available, multiple grain size data are included and the averages have been calculated. The selected grain size data associated with the current data sites show that the surficial sediments are predominantly silty clay and the mean grain sizes range from 7.2 to 8.6 Φ (0.0026 to 0.007 mm; Mean grain size in mm is equal to $2^{-\Phi}$). Bottom sediments in several sites contain significant percentages of sand.

The cores used in the erosion threshold measurements of Walker et al. (2008) were from the Beaufort mid-shelf (in 33 m water depth) and shelf break and upper slope environments (in 250 to 520 m water depths). Although grain size data of the samples were not presented, the size fraction percentage data indicated that these samples used in the erosion threshold measurements were dominantly silt and clay (80-90%) with minor percentages of sand (5-10%). In one of the earliest studies of sample compilation and grain size interpretation for the Beaufort Sea, Pelletier (1975) demonstrated that the distribution of silt and clay dominates the surficial sediments on the seabed of the Beaufort Shelf and upper slope. The grain sizes for samples in water depths of 100-600 m (over the shelf break and slope) ranged between 6.2 - 8.8 Φ (0.0022 - 0.014 mm). The mean grain size values associated with the 11 current data sites are therefore within the range of grain sizes interpreted by Pelletier (1975) and are silty clay similar to the samples used in the erosion measurements of Walker et al. (2008). Accordingly, a choice of threshold criterion $U_{100cr} = 19$ cm/s is deemed appropriate and applied for all mooring sites. Forest et al. (2016) evaluated the correlation between measured near-bed current and suspended sediment concentration on the Beaufort Shelf break (BR-B and BR-2) and estimated an envelope of threshold current speeds of 18–36 cm/s. These estimates are in qualitative agreement with the values of 19 – 31 cm/s derived using the quadratic stress law (eq. 5) in this study and the erosion threshold from laboratory experiments by Walker et al. (2008).

For all mooring data compilations, the mean, maximum and 95th percentile current speeds as well as potential sediment erosion frequency averaged annually and over multi-years where applicable, are presented in tables in the sections for each geographic areas.

Table 2 Mean grain size, sediment type percentages, and other essential information of sediment samples associated with the selected mooring data sites analyzed in this study. The sediment type data are the percentages of gravel, sand, silt and clay. Mean grain size is given in Φ and mm scales (Mean in mm is equal to $2^{-\Phi}$). Water depths marked with ~ indicate that depth data were not available from the sample stations and were estimated from the gridded bathymetry in a GIS database. The IDs in the last column are used to represent the sediment samples in the maps of each geographic areas.

Mooring Sites	Expedition	Station	Sample Type	Lat	Long	Water depth (m)	Gravel%	Sand%	Silt%	Clay%	Mud%	Mean (Φ)	Mean (mm)	ID
BR-2	70PARIZEAU	876	Grab	70.0000	-138.0333	180	0.00	0.57	23.52	75.91	99.43	8.60	0.00258	1
SS4b	70PARIZEAU	6140	Grab	69.8333	-138.5167	193	0.02	0.53	26.45	73.00	99.45	8.48	0.00280	2
AS84	70PARIZEAU	6126	Grab	70.0000	-138.4667	270	0.00	0.49	24.61	74.89	99.51	8.48	0.00280	3
BR-B	71PARIZEAU	6584	Grab	70.6817	-135.5383	146	0.01	0.32	31.06	68.61	99.67	8.40	0.00296	4
IMP85B	71PARIZEAU	6582	Grab	70.6000	-136.0850	265	0.00	3.67	23.53	72.80	96.33	8.36	0.00304	5
BR-A1	69050	5342	Piston core	70.7083	-135.8667	495	0.00	2.16	35.20	62.64	97.84	8.13	0.00357	6
I	71PARIZEAU	6604	Grab	70.8617	-134.4533	78	0.00	2.41	26.36	71.23	97.59	8.34	0.00309	7
SIC2	70021	5785	Grab	71.0278	-133.4880	~150	0.10	6.99	42.72	50.19	92.91	7.36	0.00609	8
SIC2	70021	837	Grab	71.0413	-133.4063	~130	0.03	2.05	26.49	71.43	97.92	8.29	0.00319	9
SIC2	69050	798	Grab	70.9333	-133.9917	80	0.06	0.35	29.98	69.61	99.59	8.41	0.00294	10
Average SIC2												8.02	0.00407	
CA04	69050	5363	Piston core	71.0167	-134.1167	289	0.00	20.61	28.52	50.87	79.39	7.15	0.00704	11
CA04	70021	5774	Grab	71.0020	-134.4223	158	0	2.09	33.24	64.67	97.91	8.22	0.00335	12
CA04	69050	800	Grab	71.1583	-133.1167	346	0.01	0.13	33.28	66.58	99.86	8.39	0.00298	13
Average CA04												7.92	0.00446	
CA07	69050	800	Grab	71.1583	-133.1167	346	0.01	0.13	33.28	66.58	99.86	8.39	0.00298	13
CA07	69050	5362	Grab	71.2000	-134.3750	850	0.00	0.03	32.89	67.08	99.97	8.48	0.00280	14
Average CA07												8.44	0.00289	
CA13	69050	5391	Grab	71.4450	-130.8983	300	0.35	11.61	40.24	47.80	88.04	7.36	0.00609	15
CA13	72PARIZEAU	7098	Grab	71.2667	-132.2100	241	1.22	3.71	40.38	54.69	95.07	7.66	0.00494	16
Average CA13												7.51	0.00552	

3.1.5 Possible pre-conditions affecting erosion threshold

Erosion thresholds are challenging to establish without in situ observations and there is a further possibility that seabed conditions affecting erosion threshold along the Beaufort Shelf break may be quite unique. Fresh water seepage (and generally associated methane) from permafrost melting below the seabed has been established for large regions, both at specific sites such as pingos (St Ange et al. 2014) and mud volcanoes (Paull et al. 2015a), but also more universally along the shelf-edge and on the upper slope (Gwiazda et al. 2018). Further, some sediment cores have clear evidence of re-frozen fluid at up to 40% by volume within the upper 1 m, apparently freezing as the seep approaches the seabed at minus temperatures (Paull et al. 2015b).

Observations of their thaw (in core) result in a slurry. However, the ice-containing sites are usually from targeted diapiric mounds; ambient seabed examples with ice are not known. It is speculated that the freeze-thaw cycles could limit when the sediment might be erodible and thawed sediment might be more erodible. Nevertheless, we introduce this possibility because of the strong geotechnical effect it would have on the mud; it may help explain the observed removal of tens of metres at some locations.

3.2 Near-bed currents and sediment mobility at western Beaufort Shelf-Mackenzie Trough (WBS-MT) area

Current data from three sites were analysed to assess the near-bed currents and sediment mobility for the western Beaufort Shelf-Mackenzie Trough (WBS-MT) area (Figure 3-2-1; Table 1). The three sites are respectively BR-2 representing the near-shelf break environment, and SS4b and AS84 representing the upper slope setting.

Site BR-2

Site BR-2 is near the shelf break east of the Mackenzie Trough in 154 m water depth. The bottom sediments are late Holocene mud (silty clay) deposition with a mean grain size of 0.0026 mm (Table 2). A down-looking acoustic Doppler current profiler (ADCP) was used to obtain current profile data averaged over 80 s every 1.5 hours in the bottom 10 m in 2011 and averaged over 15 s hourly in the bottom 13 m in 2012 (Table 1). In order to compare with current data measured at similar heights above bottom at other shelf-break sites on central Beaufort Sea shelf, the measured bottom current data at 10 m above bottom (mab) U10 were analyzed. The magnitude and direction of U10 for 2011-12 are shown in Figure 3-2-2 and that for 2012-13 in Figure 3-2-3. Current directions from 0° to 90° were plotted as 360° – 450° to better differentiate the dominant current directions. Statistics of mean current magnitude, 95th percentile speed, maximum current speed, and sediment erosion frequency averaged annually and for multi-years if applicable are given in Table 3. The mean 95th percentile current speed and sediment erosion frequency are also labeled next to the mooring sites in Figure 3-2-1. The maximum bottom

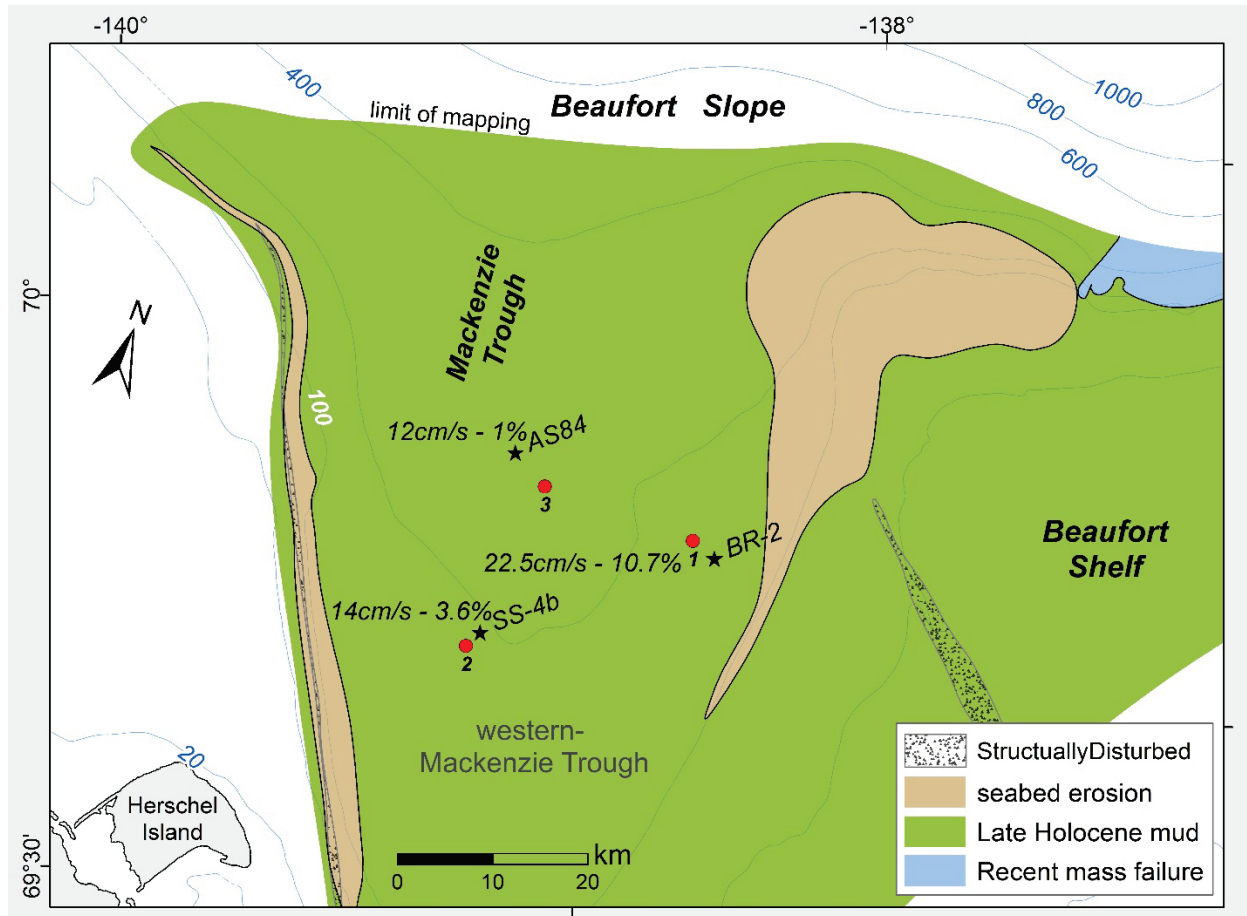


Figure 3-2-1 Map of mooring sites (stars) and associated sediment sample stations (circles; ID in Table 2) superposed on the mapped erosion and non-deposition zone for the western Beaufort Shelf-Mackenzie Trough (WBS-MT) area. The numbers next to the mooring site names are respectively the 95th percentile current speed (cm/s) and sediment erosion frequency (% of time) for that mooring site.

currents reached ~60 cm/s and the threshold for sediment erosion ($U_{100cr} = 19$ cm/s) was exceeded in 15 events in 2011-12 at BR-2. For times in which threshold was exceeded, current directions were to the NNW and NNE sectors for 66% of the time and to the SSW and SSE sectors for 33% of the time. Thus strong current events were largely to the north or south, as contour currents approximately aligned with the local bathymetry. Strong current events were evenly distributed in the summer and fall seasons. Winter and spring seasons were relatively quiescent. There were three events in which maximum bottom currents exceeded 50 cm/s. The three events occurred respectively in late October 2011, in early November 2011, and in early September 2012. The mean and 95th percentile current speeds were 8.3 and 19.3 cm/s respectively and sediment erosion occurred in 5.3% of the time.

Table 3 Statistics of mean, 95th percentile, maximum bottom current speed and sediment erosion frequency for mooring sites at the Western Beaufort Shelf-Mackenzie Trough area. Numbers in parentheses following mooring sites give the water depth of the mooring site. Mean currents in parentheses following data duration indicate the height of current data different from that shown in the column header. All currents are in cm/s and erosion frequency is in % of the time.

	Mean (U10)	95 th percentile	Maximum	Erosion Frequency
BR-2 Mackenzie Trough shelf-break (154 m)				
2011-12	8.3	19.3	57.5	5.3
2012-13	12.1	25.6	53.7	16.1
Average	10.2	22.5	55.6	10.7
SS-4b Mackenzie Trough upper slope (200 m)				
1987-88 (U6)	7.4	14.0	33.4	3.6
AS84 Mackenzie Trough upper slope (280 m)				
1984-85 (U6)	4.6	12.0	31.5	1.0
Average SS-4b, AS84	6.0	13.0	32.5	2.3

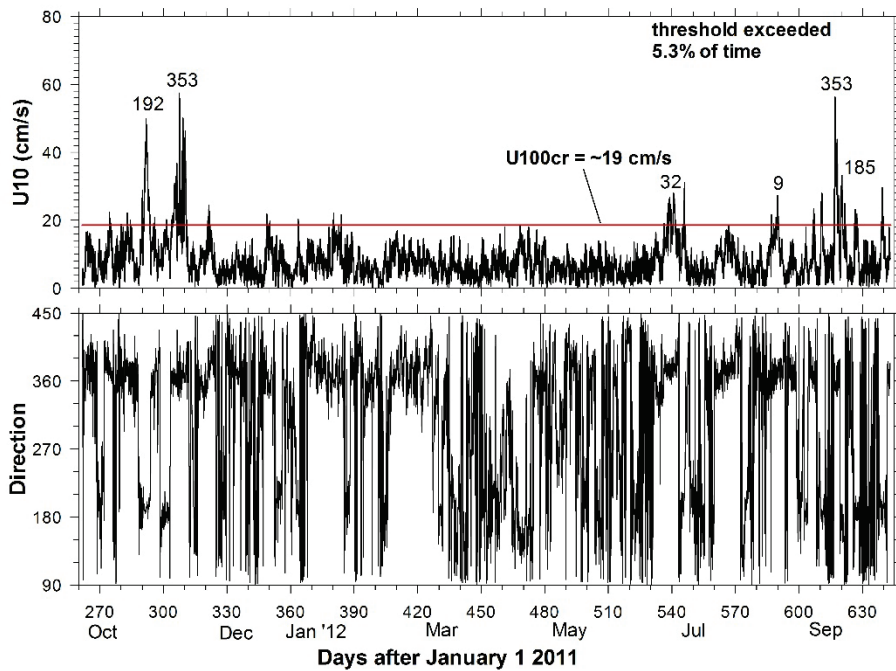


Figure 3-2-2 Magnitude and direction of bottom currents for 2011-12 at BR-2 on the shelf break east of the Mackenzie Trough. The red line represents the critical current for sediment erosion, U100cr. Numbers mark the direction of currents at the peak of current events.

In comparison to 2011-12, strong bottom current events occurred more frequently in 2012-13 and these events were more evenly distributed over all four seasons (Figure 3-2-3). Moderate events with speeds reaching 40 cm/s occurred one each in late November 2012 and early September 2013. However, the strongest events with currents greater than 50 cm/s occurred in winter 2013. The mean and 95th percentile current speeds reached 12 and 26 cm/s respectively. These were stronger than 2011-12 and resulted in sediment erosion in 16% of the time. As found for the 2011-12 data, the strong bi-directionality (either to the NNE or to the SSW) predominated the near-bed currents in 2012-13 at BR-2.

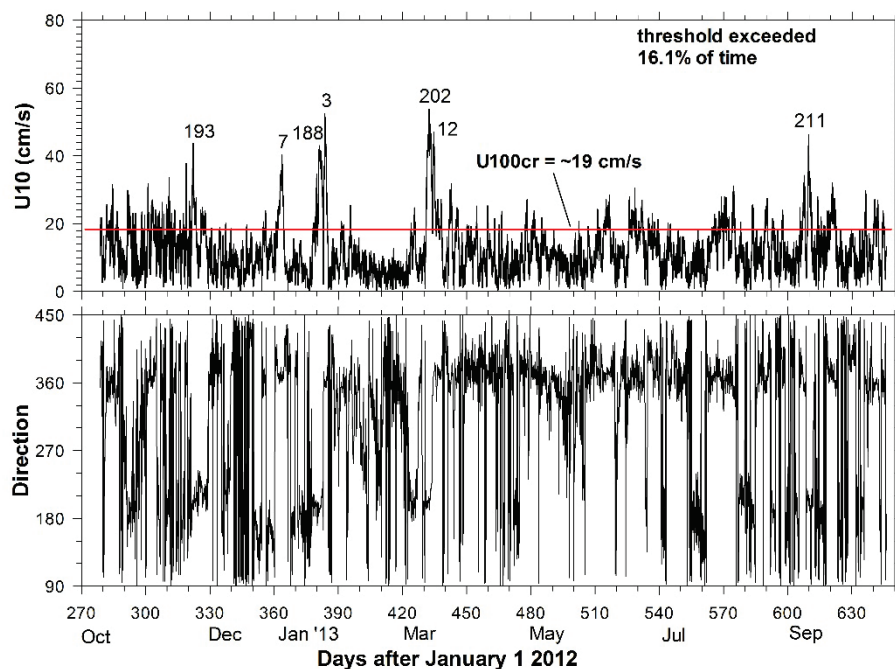


Figure 3-2-3 Magnitude and direction of bottom currents for 2012-13 at BR-2 of the shelf break east of the Mackenzie Trough. The red line represents the critical current for sediment erosion, U100cr. Numbers mark the direction of currents at the peak of current events.

Site AS84

AS84 was on the upper slope of central Mackenzie Trough in 280 m water depth (Figure 3-2-1). The bottom sediments are silty clay with a mean grain size of 0.0028 mm. A RCM4 current meter was deployed at 274 m depth to record hourly-averaged data at 6 mab from 1984/3 - 1985/8. Speed and direction of the measured currents at 6 mab (U6) are shown in Figure 3-2-4. Bottom currents reached a maximum speed of ~30 cm/s and exceeded the threshold current in 8 events for this deployment. These events mainly occurred in the fall 1984, winter and summer 1985. Currents were weak in summer 1984 and in the spring of both years. Current directions at

the peaks of the strong current events were predominantly to the NNW sector and secondary directions were to the SE and SW sectors. The mean, 95th percentile and maximum currents at this slope site all were lower than BR-2 on the shelf break (Table 3). As a result, sediment erosion potential was only 1% of the time.

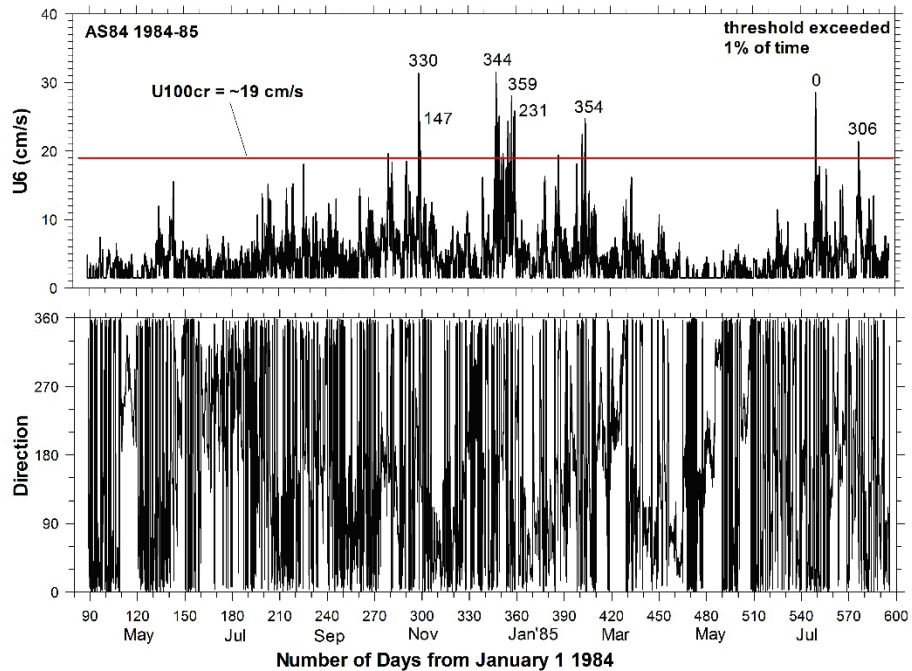


Figure 3-2-4 Magnitude and direction of bottom currents for 1984-85 at AS84 on the upper slope of central Mackenzie Trough. The red line represents the critical current for sediment erosion, U100cr. Numbers mark the direction of currents at the peak of current events.

Site SS4b

SS4b site was on the upper slope of central Mackenzie Trough in 200 m water depth (Figure 3-2-1). The bottom sediments are silty clay with a mean grain size of 0.0028 mm. A RCM4 current meter was deployed at 150 m depth to record hourly-averaged data for 7 months from 1987/8 to 1988/3. To be compatible with the data at AS84 site, the measured current data at 50 mab were extrapolated to 6 mab. The magnitude and direction of the extrapolated bottom current are shown in Figure 3-2-5. Threshold current was exceeded in 12 events with maximum currents reaching > 30 cm/s. The directions of bottom currents under the condition of threshold exceedance were variable: 48% to the SW, 26% to the SE and 25% to the NW. However, the currents in the strongest event in mid-January 1988 were to the NW. The mean, 95th percentile and maximum currents were 7.4, 14 and 33 cm/s respectively and were moderately higher than that at AS84 to resulting in potential sediment erosion in 3.6% of the time.

Despite the different depths, SS4b and AS84 sites are both on the upper slope. The averaging of the statistics from these two sites gives mean current speed of 6 cm/s, 95th percentile speed of 13 cm/s and erosion frequency at 2.3% (Table 3). The mean and 95th percentile current speeds averaged for 2011-2013 at BR-2 are respectively 10.2 and 22.5 cm/s and these caused sediments potentially to be eroded in 10.7% of the time. This comparison would suggest that bottom current intensity and sediment mobility decrease from the shelf break to the upper slope for the WBS-MT area.

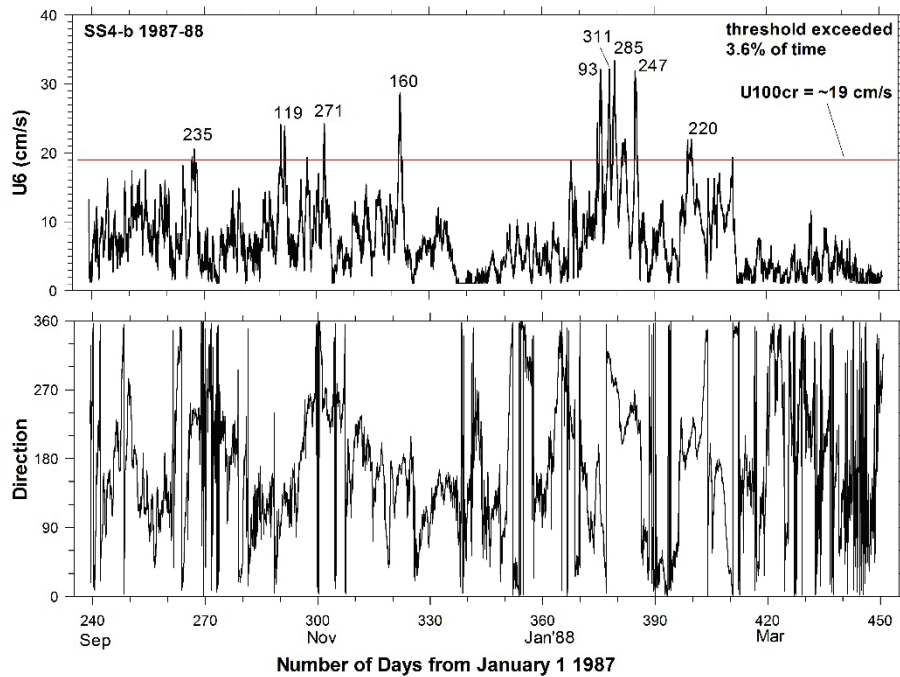


Figure 3-2-5 Magnitude and direction of bottom currents for 1987-88 at SS4b on the upper-most slope of central Mackenzie Trough. The red line represents the critical current for sediment erosion, U100cr. Numbers mark the direction of currents at the peak of current events.

3.3 Near-bed currents and sediment mobility at western Central Beaufort Shelf (WCBS) area

Current data from four sites were analysed to assess the near-bed currents and sediment mobility for the western Central Beaufort Shelf (WCBS) area (Figure 3-3-1; Table 1). The four mooring sites are respectively BR-B near the shelf break, IMP85B on the upper slope, BR-A1 on the middle slope, and I on the outer shelf.

Site BR-B

Site BR-B is near the shelf break of the western Central Beaufort Shelf in 156 m water depth. The site is at the boundary between the erosion zone and late Holocene mud and the bottom sediments are silty clay with a mean grain size of 0.0030 mm. In 2009-2011, ADCP profilers at ~140 m depth recorded continuous 20 minute average data respectively at 35 mab (2009) and 25 mab (2010) (Table 1). For 2011-2013, down-looking ADCPs at ~140 m depth provided current profiles (averaged for 360 s every 2 hours in 2011 and for 280 s every hour in 2012) for the bottom 13 m above seabed. Because currents were measured at 11 mab at the slope site IMP85B in 1985 (Table 1), current data at BR-B were extrapolated to or picked at 11 mab to ensure compatible current measurement heights at various sites. The magnitude and direction of bottom currents U11 at BR-B for 2009, 2010, 2011, and 2012 are presented in Figures 3-3-2, 3-3-3, 3-3-4 and 3-3-5 respectively. Statistics of mean, 95th percentile, and maximum current speeds and sediment erosion frequency are listed in Table 4. The average 95th percentile current speed and sediment erosion frequency are also labeled next to the mooring sites in Figure 3-3-1.

Figure 3-3-2 shows that maximum currents reached greater than 60 cm/s and bottom currents frequently exceeded the threshold for sediment erosion in 2009-10. The directions of peak currents were predominantly to the NE. Bottom currents were weaker in spring 2010 (March to May) and were typically less than 20 cm/s. Bottom currents exceeded the threshold speed with roughly equal frequencies for summer, fall, and winter seasons. However, the strongest current events respectively occurred in mid-October 2009 (52 cm/s), mid-January (63 cm/s) and mid-February (53 cm/s) of 2010 and currents at the peaks of these events were all to the ENE. The mean and 95th percentile current speeds reached 11 and 30 cm/s respectively and caused potential sediment erosion in 17% of the time. Bottom current data in 2010-11 (Figure 3-3-3) demonstrate that the maximum currents reached ~54 cm/s and bottom currents frequently exceeded the threshold for sediment erosion. Strong bottom currents were predominantly to the ENE (84%). The frequency of threshold exceedance was similar for all four seasons, although stronger current events mostly occurred in the ice-covered winter conditions (mid-late November to mid-March). The mean and 95th percentile current speeds were 11 and 26 cm/s respectively and caused potential sediment erosion in 16% of the time.

The maximum bottom currents reached nearly 49 cm/s and again exceeded the threshold frequently in 2011-12 (Figure 3-3-4). For time when threshold was exceeded, currents were to the NE for 83% of the time and to the SW for 10% of the time. There were no significant differences in the threshold exceedance frequency in different seasons. However, the two strongest current events respectively occurred in early November 2011 (~49 cm/s to 56°) and mid-September 2012 (45 cm/s to 66°). Unlike 2009 and 2010, currents during the ice-covered winter months in 2011 were not particularly energetic. Mean and 95th percentile current speeds were 10.6 and 22 cm/s respectively. These were moderately lower than those in 2009 and 2010

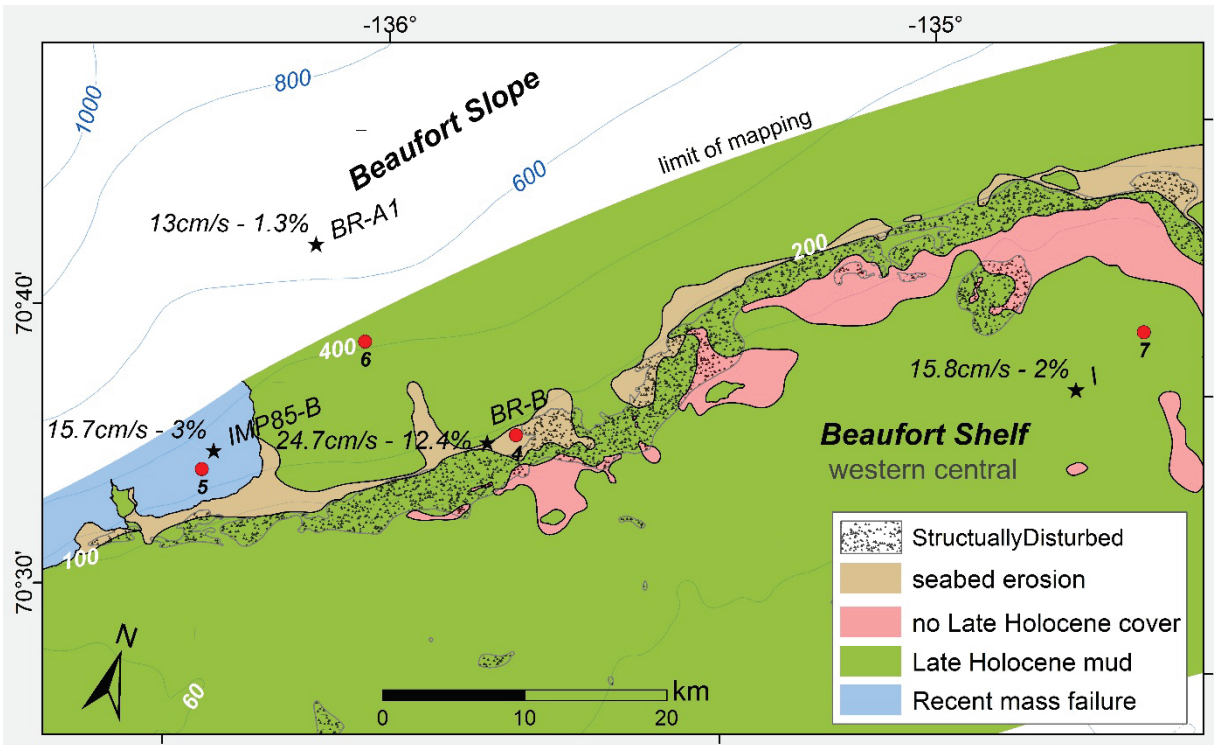
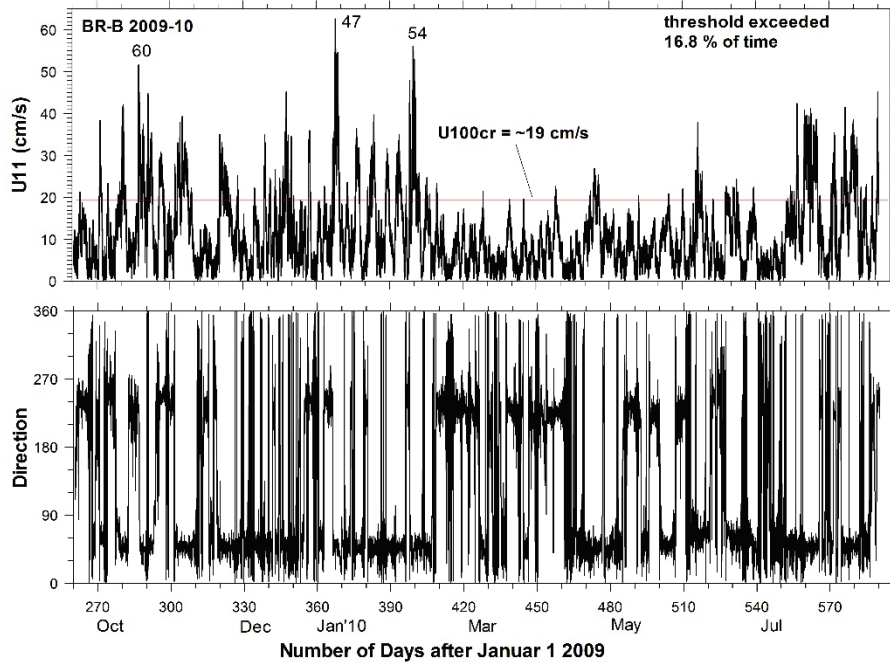


Figure 3-3-1 Map of mooring sites (stars) and associated sediment sample stations (circles; ID in Table 2) superposed on the mapped erosion and non-deposition zone for the western Central Beaufort Shelf (WCBS) area. The numbers next to the mooring site names are respectively the 95th percentile speed (cm/s) and sediment erosion frequency (% of time) for that mooring site.

and therefore potentially caused sediment erosion for 10% of the time. The magnitude and direction of measured bottom currents for 2012-13 are presented in Figure 3-3-5 which shows that maximum bottom current reached 43 cm/s and that bottom currents exceeded the threshold much less frequently than the previous three years. Currents during the strong current events were again predominantly to the NE (84% of the time). Currents in the spring were the weakest. Currents became stronger and the frequency of threshold exceedance also increased in the summer and fall seasons. However, the strongest current event occurred in late January 2013. The mean and 95th percentile current speeds were 9.5 and 21 cm/s respectively. These were the lowest over the 4 year period of 2009-13 and correspondingly the bottom currents resulted in sediment erosion in only 7% of the time (Table 4).

Site IMP85B

IMP85B site was on the upper slope of the WCBS area in 302 m water depth (Figure 3-3-1). The site is over a mass failure with no late Holocene cover. Bottom samples suggest a thin layer of



Figures 3-3-2 Magnitude and direction of bottom currents for 2009-10 at BR-B on the shelf break of the western Central Beaufort Shelf area. The red line represents the critical current for sediment erosion, U100cr. Numbers mark the direction of currents at the peak of current events.

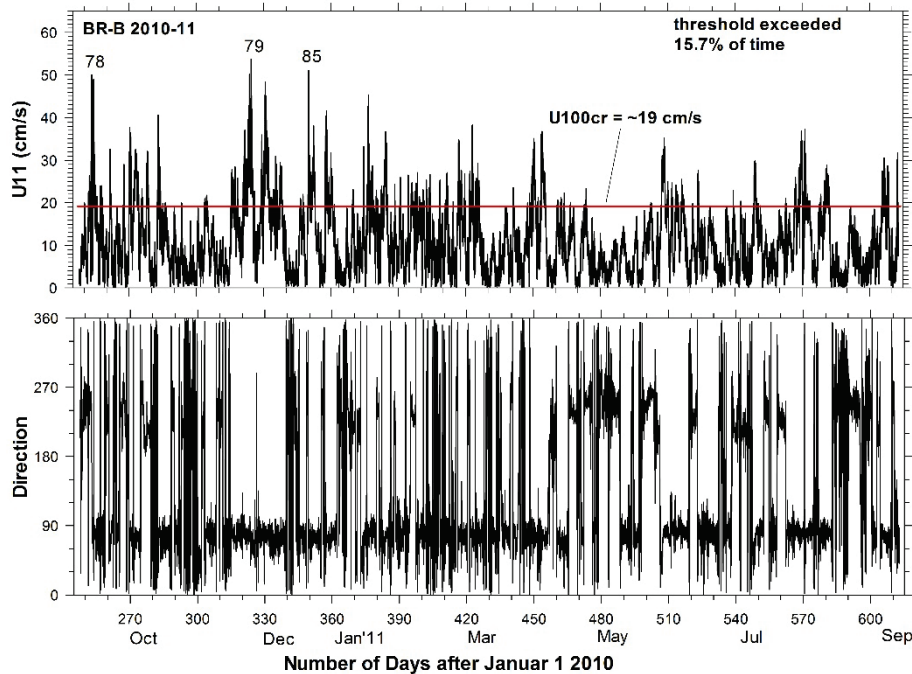


Figure 3-3-3 Magnitude and direction of bottom currents for 2010-11 at BR-B on the shelf break of the western Central Beaufort Shelf area. The red line represents the critical current for sediment erosion, U100cr. Numbers mark the direction of currents at the peak of current events.

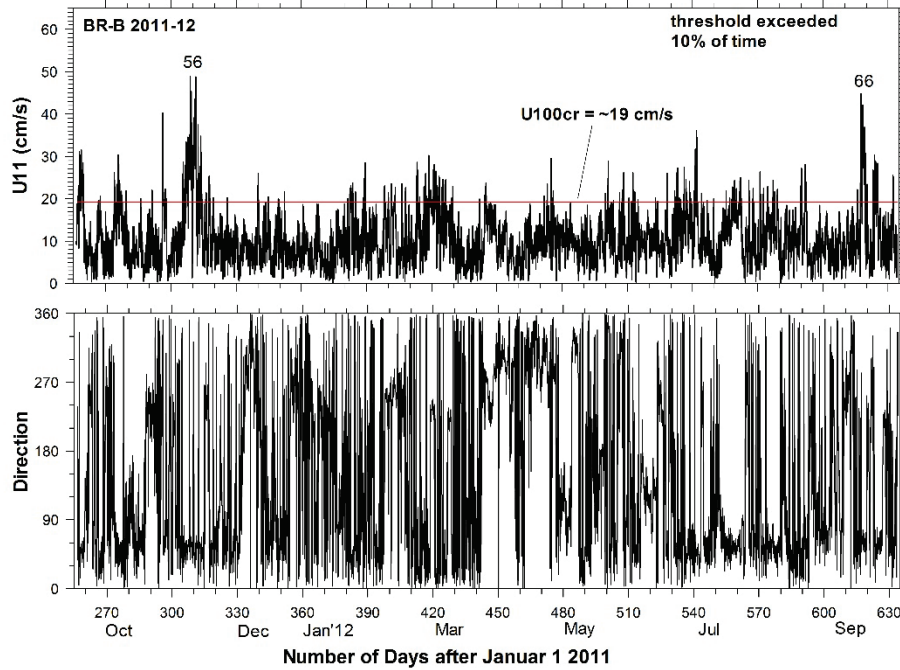


Figure 3-3-4 Magnitude and direction of bottom currents for 2011-12 at BR-B on the shelf break of the western Central Beaufort Shelf area. The red line represents the critical current for sediment erosion, U100cr. Numbers mark the direction of currents at the peak of current events.

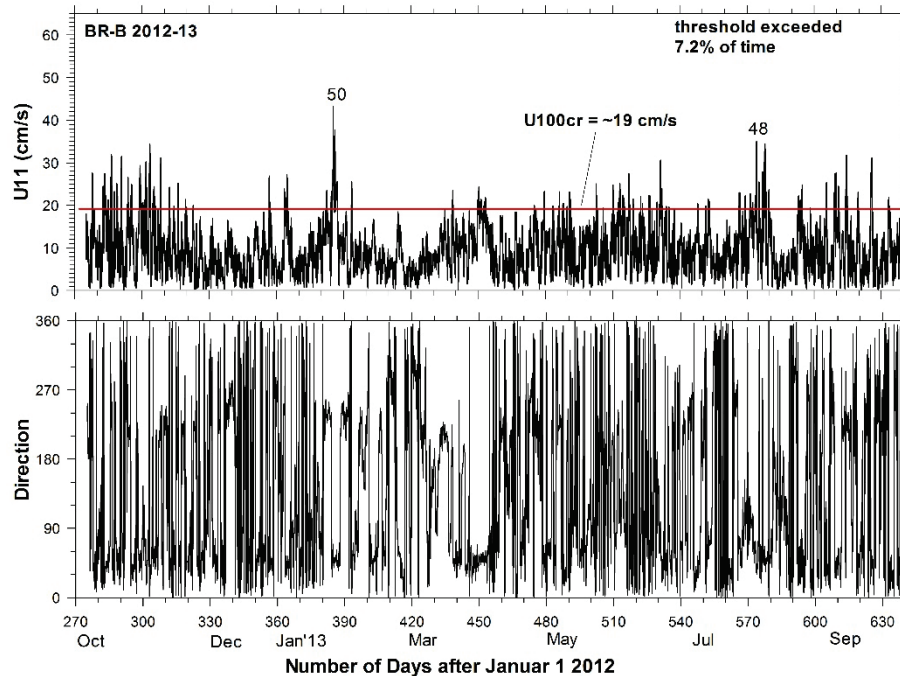


Figure 3-3-5 Magnitude and direction of bottom currents for 2012-13 at BR-B on the shelf break of the western Central Beaufort Shelf area. The red line represents the critical current for sediment erosion, U100cr. Numbers mark the direction of currents at the peak of current events.

Table 4 Statistics of mean, 95th percentile, maximum bottom current speed and sediment erosion frequency for mooring sites at the Western Central Beaufort Shelf area. All currents are in cm/s and erosion frequency is in % of the time.				
	Mean (U11)	95 th percentile	Maximum	Erosion Frequency
I outer shelf site (75 m)				
2009-10	7.5	16.2	31.6	2.1
2010-11	7.2	15.4	34.8	1.8
Average	7.4	15.8	33.2	2.0
BR-B shelf break (156 m)				
2009-10	11.2	29.5	62.6	16.8
2010-11	11.0	26.2	53.8	15.7
2011-12	10.6	22.4	48.9	10.0
2012-13	9.5	20.6	43.2	7.2
Average	10.6	24.7	52.1	12.4
(Avg. 2011-13)	10.1	21.5	46.1	8.6
IMP85B upper slope (302 m)				
1985-86	5.6	15.7	58.4	3.0
BR-A1 slope (660 m)				
2009-10 (U16)	4.8	12.2	30.7	1.1
2010-11 (U14)	5.0	12.1	24.4	1.2
2011-12 (U12)	5.3	13.9	28.2	1.3
2012-13 (U13)	5.6	13.7	40.9	1.6
Average	5.2	13.0	31.1	1.3

sandy silty clay with a mean grain size of 0.0030 mm. A RCM4 current meter was deployed at 291 m depth (11 mab) to record hourly-averaged current data from 1985/4 to 1986/4. The bottom current at 11 mab U11 (Figure 3-3-6) indicates that maximum bottom currents reached ~60 cm/s and there were ~19 events in which the threshold was exceeded. For these events, currents were predominantly to the NE (92% of the time). Currents were relatively weak in the spring. Bottom currents exceeded the threshold in roughly equal frequencies for the summer, fall and winter seasons. However, the two strongest events with current speeds >45 cm/s occurred in mid-November and early December 1985 in ice-covered winter conditions. The mean and 95th percentile current speeds were 5.6 and 16 cm/s respectively and sediment was eroded for 3% of the time over the mooring duration (Table 4).

Site BR-A1

BR-A1 is located on the middle slope of the western central Beaufort Shelf area in ~660 m water depth (Figure 3-3-1). The bottom sediments are sandy silty clay with a mean grain size of 0.0036 mm. In 2009-2011, DVS current meters were moored at ~670 m depth to measure currents of

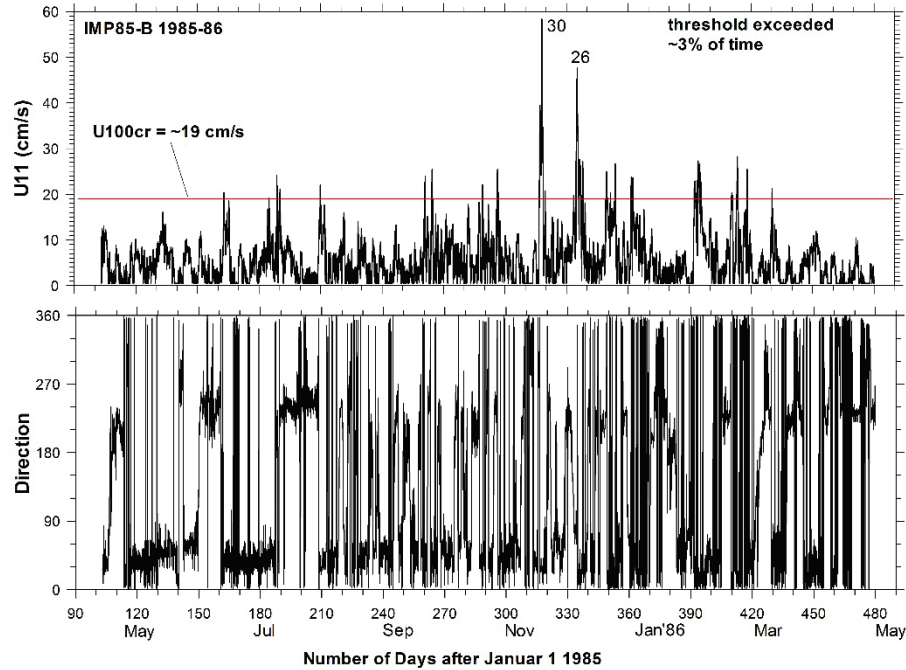
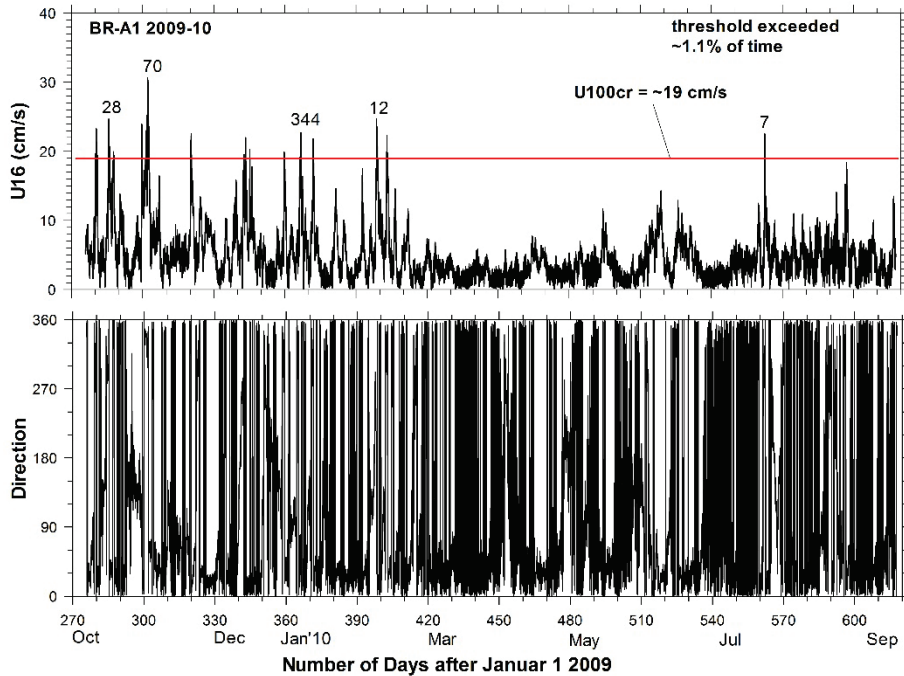


Figure 3-3-6 Magnitude and direction of bottom currents for 1985-86 at IMP85B on the upper slope of the western Central Beaufort Shelf area. The red line represents the critical current for sediment erosion, U100cr. Numbers mark the direction of currents at the peak of current events.

continuous 20 minute (30 minute in 2010) averages at 14–16 m above bottom (Table 1). In 2011-2013, Aquadop Deepwater current meters deployed at ~647 m depth recorded hourly data averaged over 120 s (2011) and half-hourly data averaged over 240 s (2012) at ~13 m above bottom. The magnitude and direction of the bottom currents at BR-A1 for each of these four years are presented in Figures 3-3-7, 3-3-8, 3-3-9 and 3-3-10 respectively. Statistics of mean, 95th percentile, and maximum current speeds and sediment erosion frequency are listed in Table 4.

The bottom current data at 16 mab in 2009 (Figure 3-3-7) demonstrates that currents were generally lower than 30 cm/s and there were 11 events in which threshold was exceeded. Currents in the hours when threshold was exceeded were predominantly to the NE (83%) and currents in the other times were to the NW (17%). Bottom currents were the weakest in the spring 2010 and slightly increased to cause occasional sediment erosion in the summer. Bottom currents were moderately stronger in the fall and winter seasons with roughly equal frequency of threshold exceedance. However, the strongest current event, ~31 cm/s to ENE, occurred in early November 2009 during the period of rapid ice formation. The mean and 95th percentile current speeds were 4.8 and 12 cm/s respectively and sediment erosion occurred in just 1.1% of the time. The bottom currents measured at 14 mab in 2010-11 were generally smaller than 25 cm/s and



Figures 3-3-7 Magnitude and direction of bottom currents for 2009-10 at BR-A1 on the slope of the western Central Beaufort Shelf area. The red line represents the critical current for sediment erosion, U100cr. Numbers mark the direction of currents at the peak of current events.

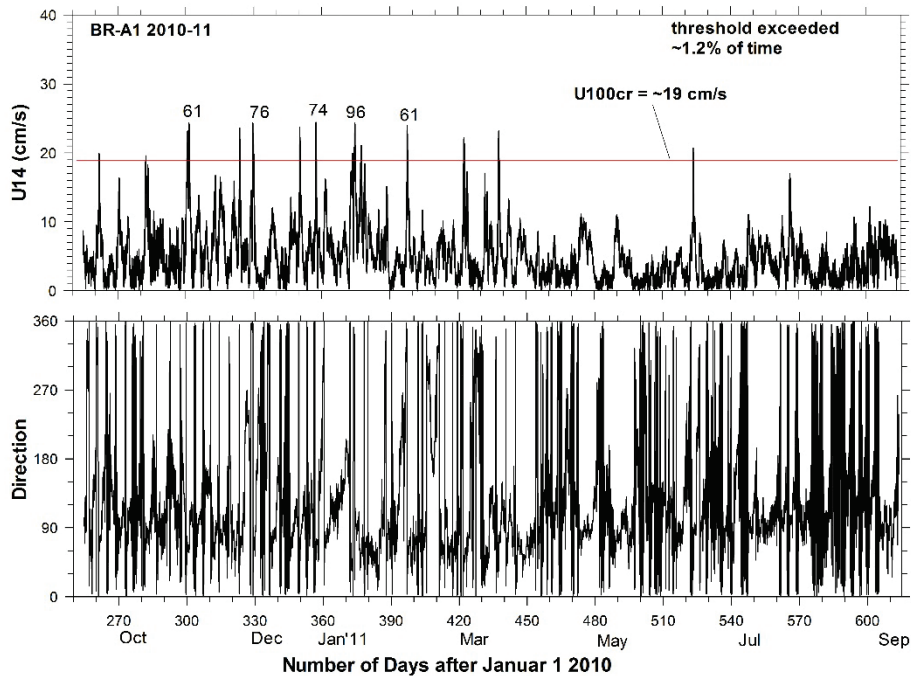


Figure 3-3-8 Magnitude and direction of bottom currents for 2010-11 at BR-A1 on the slope of the western Central Beaufort Shelf area. The red line represents the critical current for sediment erosion, U100cr. Numbers mark the direction of currents at the peak of current events.

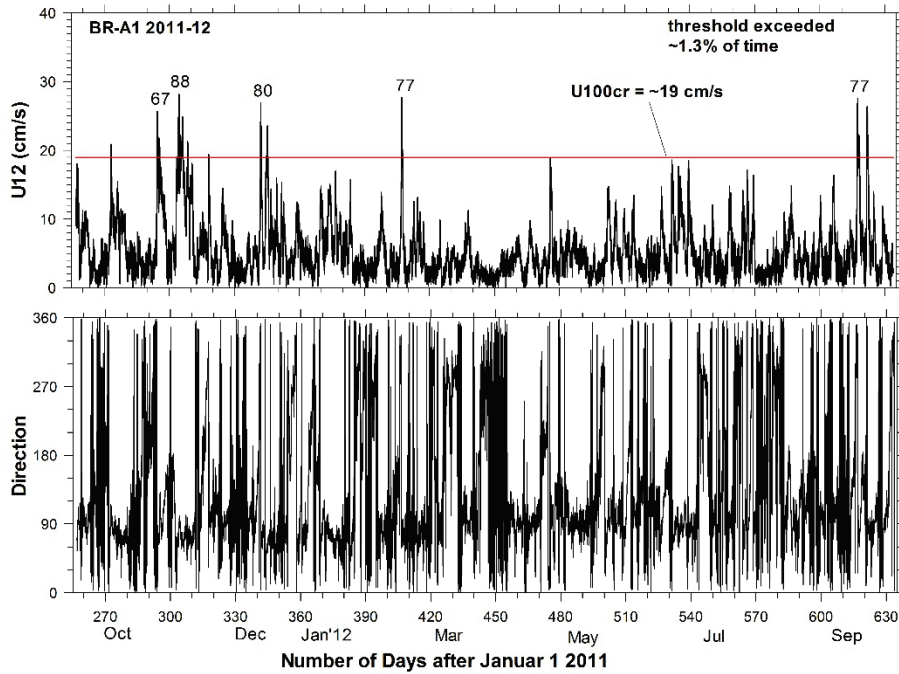


Figure 3-3-9 Magnitude and direction of bottom currents for 2011-12 at BR-A1 on the slope of the western Central Beaufort Shelf area. The red line represents the critical current for sediment erosion, U100cr. Numbers mark the direction of currents at the peak of current events.

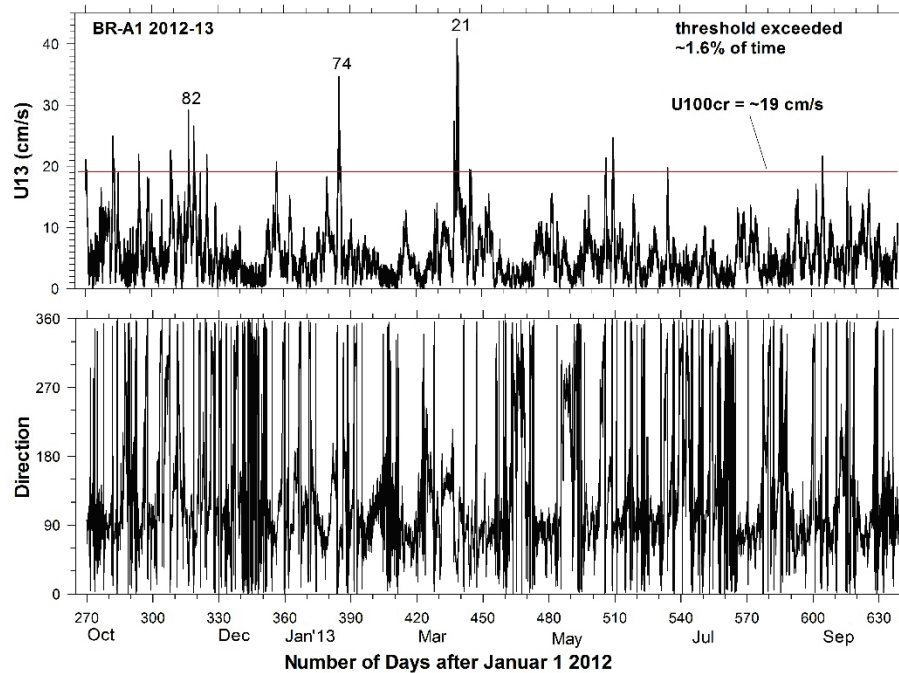


Figure 3-3-10 Magnitude and direction of bottom currents for 2012-13 at BR-A1 on the slope of the western Central Beaufort Shelf area. The red line represents the critical current for sediment erosion, U100cr. Numbers mark the direction of currents at the peak of current events.

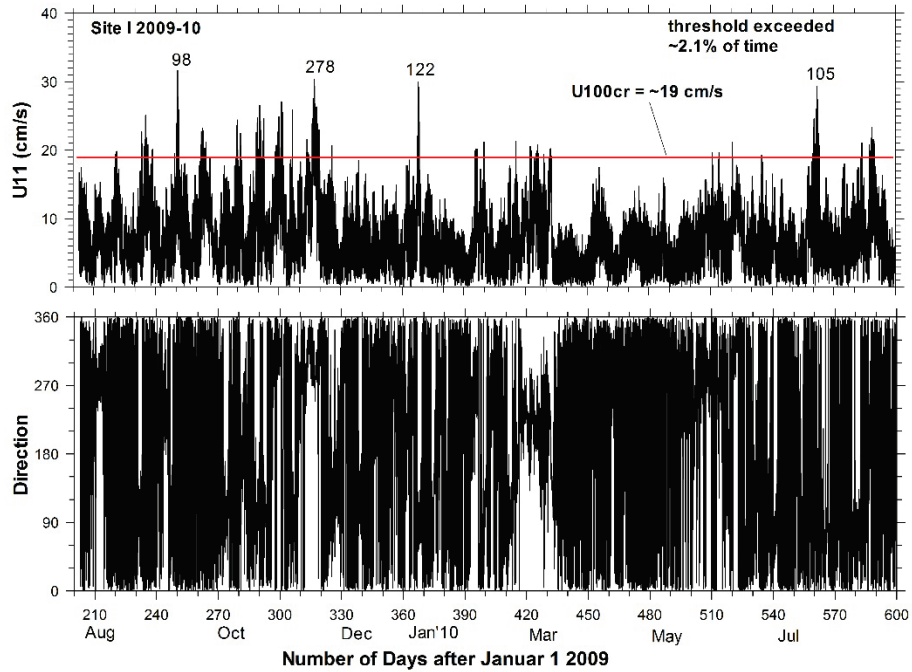
showed 13 events in which threshold was exceeded (Figure 3-3-8). For the hours when erosion occurred, the currents were to the ENE for 80% of the time and currents in the other hours were to the ESE (20% of the time). The temporal variations demonstrated a similar pattern to that of 2009-10, i.e. the bottom currents in spring and summer were weak and rarely exceeded the threshold. Currents in the fall and winter were moderately stronger and associated with nearly equal frequency of sediment erosion. The mean and 95th percentile current speeds were 5 and 12 cm/s respectively and sediment erosion occurred in 1.2% of the time.

The current data measured at 12 mab in 2011-12 are shown in Figure 3-3-9. Maximum currents were <30 cm/s and there were 9 events in which threshold current was exceeded. For the hours when threshold was exceeded, bottom currents were predominantly to the ENE (89% of the time) and the currents were to the ESE in 11% of the time. Currents in the spring and summer were weaker than the fall and winter and did not exceed the threshold required for sediment erosion. The majority of the current events (6 out of the 9 events) strong enough to cause sediment erosion occurred in the fall. The mean and 95th percentile current speeds were 5.3 and 14 cm/s respectively and sediment erosion occurred in 1.3% of the time. Bottom currents were the strongest in 2012-13 as the maximum currents measured at 13 mab reached 41 cm/s and the threshold current was exceeded in 15 events (Figure 3-3-10). For hours when the threshold was exceeded, currents were mostly to the ENE (66% of the time) and to the ESE (22% of the time). Bottom currents in the spring and summer were weaker than that in the fall and winter. Although several events of sediment erosion occurred in the spring and summer, the majority of the sediment erosion events occurred in the fall and the strongest events with current speed exceeding ~30 cm/s occurred in the winter months (late January and mid-March) of 2013. The mean and 95th percentile current speeds were 5.6 and 14 cm/s respectively and sediment erosion occurred in 1.6% of the time.

Site I

Site I represented the outer shelf setting in 75 m water depth of the WCBS area (Figure 3-3-1). The bottom sediments are sandy silty clay with a mean grain size of 0.0031 mm. The data from this site was included and analyzed to demonstrate current magnitude and erosion frequency on the outer shelf shoreward from the central Beaufort Sea shelf break. ADCP profilers were deployed to collect continuous current data averaged for 15 minutes at 26 m (in 2009-10) and 31 m (in 2010-11) above bottom. Per the rationale described for the BR-B data, the measured current data were extrapolated to 11 mab. The extrapolated bottom current data are presented in Figures 3-3-11 and 3-3-12 respectively. Statistics of mean, 95th percentile, and maximum current speeds and sediment erosion frequency are listed in Table 4.

The extrapolated bottom currents at 11 mab for 2009-10 (Figure 3-3-11) exceeded the threshold speed in ~23 events and the current directions for events with peak currents > 30 cm/s were



Figures 3-3-11 Magnitude and direction of bottom currents for 2009-10 at Site I on the outer shelf of the western Central Beaufort Shelf area. The red line represents the critical current for sediment erosion, U100cr. Numbers mark the direction of currents at the peak of current events.

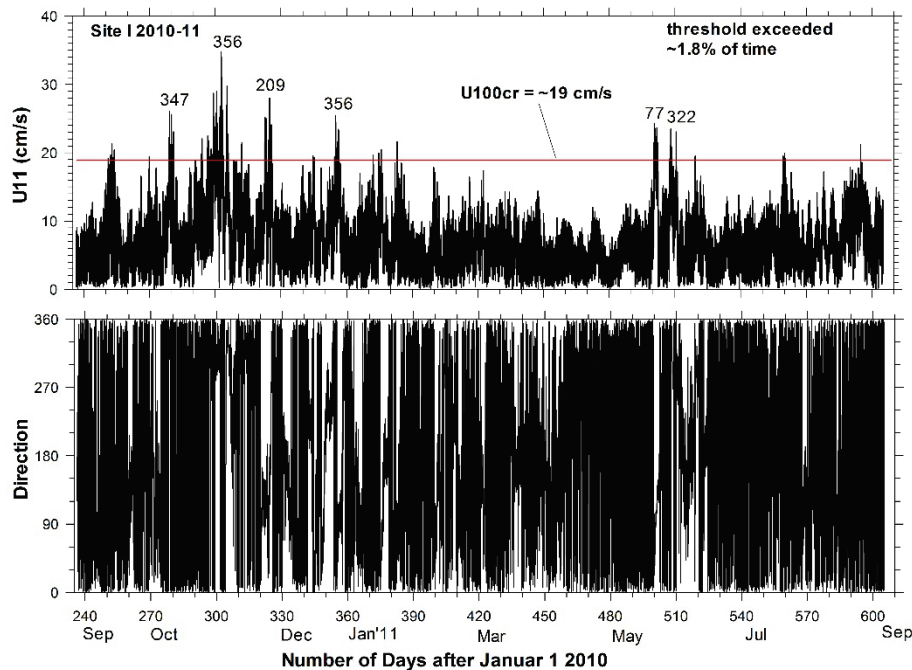


Figure 3-3-12 Magnitude and direction of bottom currents for 2010-11 at Site I on the outer shelf of the western Central Beaufort Shelf area. The red line represents the critical current for sediment erosion, U100cr. Numbers mark the direction of currents at the peak of current events.

either to the ESE or to the west. However, current direction varied widely (omnidirectional) with 42% to the NW, 28.5% to the SE, 24% to the NE, and 6% to the SW. Currents in the fall and winter were generally stronger than in the spring and summer. The mean and 95th percentile current speeds were 7.5 and 16 cm/s respectively and the sediment erosion frequency was 2.1% of the time. The extrapolated bottom currents for 2010-11 are presented in Figure 3-3-12 which demonstrates that bottom currents exceeded the threshold in ~15 events. Detailed analysis of the current directions for hours in which threshold was exceeded indicates that currents were omnidirectional with 48% to the NW, 26% to the NE, 23% to the SE, and 3% to the SW. Although transport occurred in all seasons, the strongest currents occurred dominantly in late fall and early winter of 2010 with current directions being dominantly to the north and the NW. The mean and 95th percentile current speeds were 7.2 and 15 cm/s respectively and the sediment was eroded in 1.8% of the time. In comparison with the shelf-beak site BR-B, magnitude of bottom currents and sediment erosion frequency both decrease at the outer shelf site I. Currents under threshold exceedance conditions were more omnidirectional at site I while currents were predominantly to the NE on the shelf break at BR-B.

3.4 Near-bed currents and sediment mobility at eastern Central Beaufort Shelf (ECBS) area

Current data from three sites were analysed to assess the near-bed currents and sediment mobility for the eastern Central Beaufort Shelf (ECBS) area (Figure 3-4-1; Table 1). The three sites are respectively SIC2 near the shelf break, CA04 on the upper slope, and CA07 on the middle slope of the ECBS area.

Site SIC2

SIC2 is near the shelf break of the eastern central Beaufort Shelf area in 111 m water depth which is quite shallower than the other shelf break sites (BR-2 and BR-B). The site is over the late Holocene mud. The three associated bottom sediment samples suggest sandy silty clay with an average mean grain size of 0.0041 mm. ADCP profilers were moored at ~107 m depth and recorded continuous 40-min averaged current data at 8 mab. The magnitude and direction of measured bottom currents at 8 mab at SIC2 for 2010, 2011, and 2012 are presented in Figures 3-4-2, 3-4-3 and 3-4-4 respectively. Statistics of mean, 95th percentile and maximum current speeds and sediment erosion frequency are listed in Table 5.

The bottom currents for 2010-11 (Figure 3-4-2) demonstrates that there were 17 events in which bottom currents exceeded the threshold speed. Currents in these sediment erosion events were predominantly to the NE (92%). The strongest events with speeds >35 cm/s occurred respectively in late November 2010 and in late February 2011 with eastward direction. Currents in spring and summer were weaker than in fall and winter and rarely exceeded the threshold for

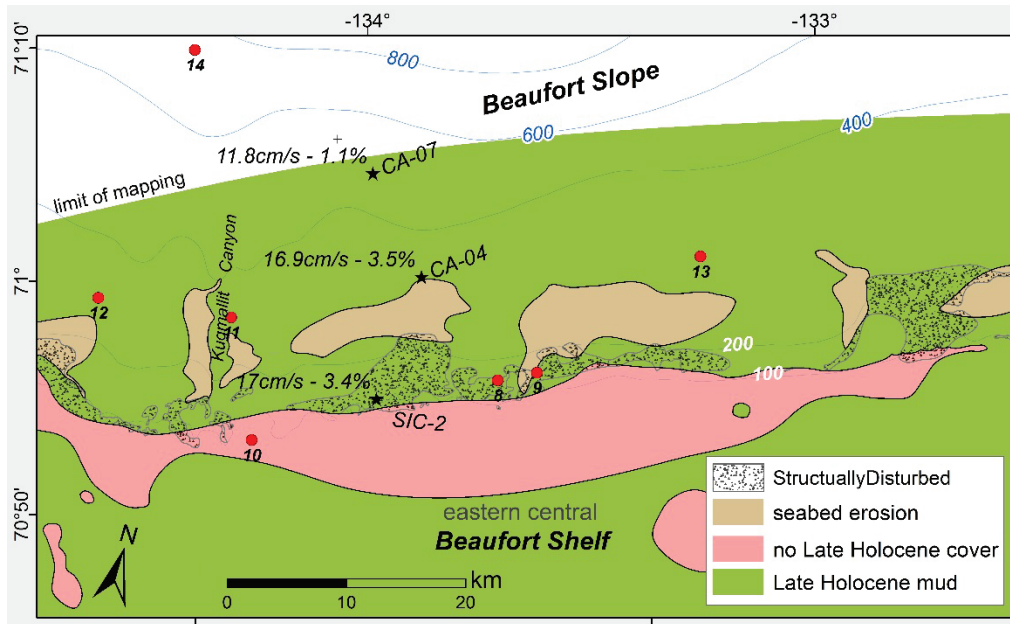


Figure 3-4-1 Map of mooring sites (stars) and associated sediment sample stations (circles; ID in Table 2) superposed on the mapped erosion and non-deposition zone for the eastern Central Beaufort Shelf (ECBS) area. The numbers next to the mooring site names are respectively the 95th percentile speed (cm/s) and sediment erosion frequency (% of time) for that mooring site.

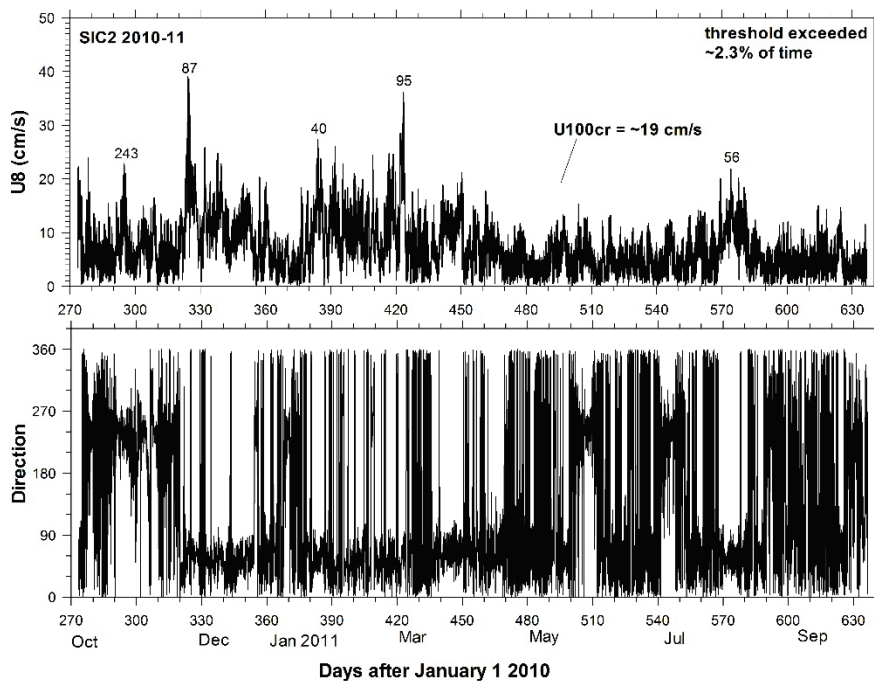


Figure 3-4-2 Magnitude and direction of measured bottom currents for 2010-11 at SIC2 on the shelf break of the eastern Central Beaufort Shelf (ECBS) area. The red line represents the critical current for sediment erosion, U100cr. Numbers mark the direction of currents at the peak of current events.

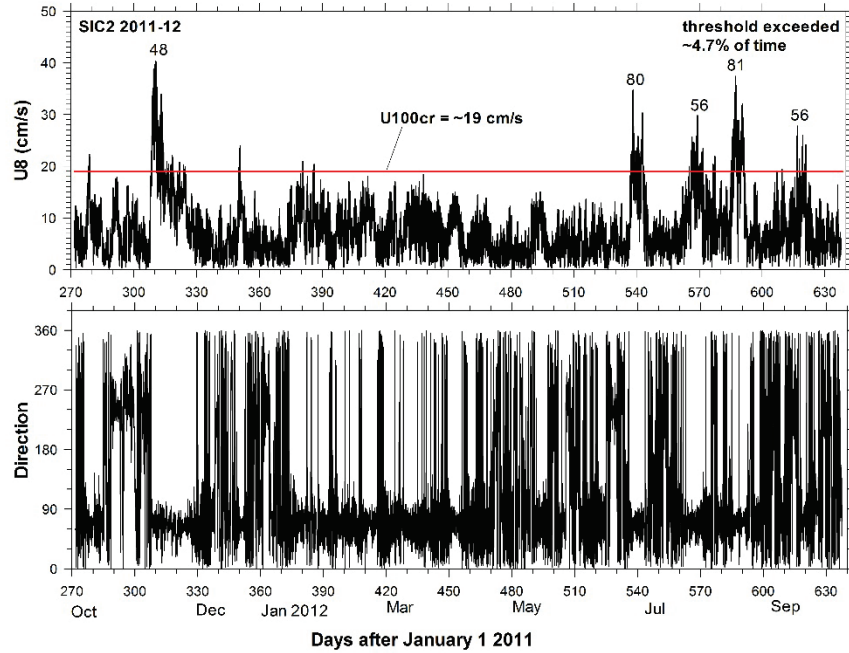


Figure 3-4-3 Magnitude and direction of measured bottom currents for 2011-12 at SIC2 on the shelf break of the eastern Central Beaufort Shelf (ECBS) area. The red line represents the critical current for sediment erosion, U100cr. Numbers mark the direction of currents at the peak of current events.

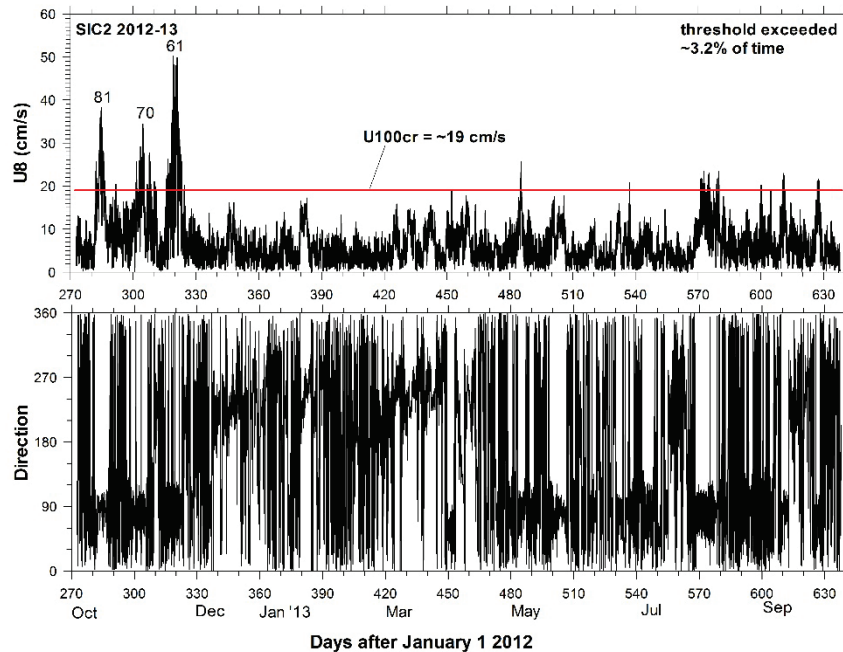


Figure 3-4-4 Magnitude and direction of measured bottom currents for 2012-13 at SIC2 on the shelf break of the eastern Central Beaufort Shelf (ECBS) area. The red line represents the critical current for sediment erosion, U100cr. Numbers mark the direction of currents at the peak of current events.

Table 5 Statistics of mean, 95th percentile, maximum bottom current speed and sediment erosion frequency for mooring sites at the eastern central Beaufort Shelf area. Standard errors are calculated for annual 95th percentile current speed and sediment erosion frequency for sites for which data are available for at least 3 years. All currents are in cm/s and erosion frequency is in % of the time.

	Mean U8	95 th percentile	Maximum	Erosion Frequency
SIC2 shelf break (111 m)				
2010-11	7.3	16.1	39.1	2.3
2011-12	8.0	18.7	40.3	4.7
2012-13	6.8	16.2	50.3	3.2
Average	7.4	17.0	43.2	3.4
Std. Error		0.85		0.7
CA04 upper slope (300 m)				
2003-04	5.6	14.7	58.8	2.2
2004-05	6.9	20.6	76.4	6.2
2005-06	6.2	15.4	51.9	2.1
Average	6.2	16.9	62.4	3.5
(Avg. 2003-05)	6.3	17.7	67.6	4.2
Std. Error		1.86		1.35
CA07 slope (500 m)				
2003-04	3.9	9.7	31.2	0.8
2004-05	4.5	13.8	37.5	1.3
Average	4.2	11.8	34.4	1.1

sediment erosion. The mean and 95th percentile current speeds were 7.3 and 16 cm/s respectively and the sediment erosion frequency was 2.3% of the time. The bottom currents for 2011-12 (Figure 3-4-3) show that the maximum current speed reached ~40 cm/s and that the threshold was exceeded in 13 events. Currents in times when threshold was exceeded were dominantly to the NE (96%). Currents in the spring were again weak. In contrast to 2010, however, currents in winter were quiescent and currents were strong in the summer. Currents reached 30-40 cm/s and were dominantly to the ENE in several events in the summer 2012. The strongest event, however, occurred in early November 2011 with northeastward currents of ~40 cm/s. The more energetic conditions of 2011 were also reflected in the mean and 95th percentile current speeds at 8 and 19 cm/s respectively which corresponded with sediment erosion in 4.7% of the time, double of 2010-11. The bottom currents for 2012-13 (Figure 3-4-4) show that the maximum current speed reached ~50 cm/s and that there were 14 events in which the threshold speed was exceeded. Currents in times when threshold was exceeded were quite variable but were dominantly to the NE (63%) and to the ESE (35%). Currents were to the southwest in only 6 sampling bursts (1%). Currents in both the winter and spring of 2013 were quiescent and were slightly stronger in the summer 2013 to cause several weak sediment transport events. The strongest events occurred in October and November 2012 in which current speeds reached 35-50

cm/s and were to the ENE. The mean and 95th percentile current speeds were 6.8 and 16 cm/s respectively and sediment erosion occurred in 3.2% of the time.

Site CA04

CA04 is on the upper slope of the eastern central Beaufort Shelf area in 300 m water depth. The site is also over the late Holocene mud but close to the northern edge of the erosion zone. The 3 associated bottom sediment samples show variable sand percentages and mean grain sizes that range 0.003 – 0.007 mm. The average of the 3 samples suggests sandy silty clay with an average mean grain size of 0.0045 mm. RCM11 current meters were deployed at ~200 m depth to collect hourly or half-hourly current data at ~100 m above bottom for 2003 – 2006. The measured current data at ~100 mab were extrapolated to that at 8 mab. The extrapolated bottom current data are presented in Figures 3-4-5, 3-4-6 and 3-4-7 respectively. The statistics of mean, 95th percentile, and maximum current speeds and sediment erosion frequency are listed in Table 5.

The magnitude and direction of the extrapolated bottom currents for 2003-04 (Figure 3-4-5) demonstrates that the maximum current speed reached ~60 cm/s and that there were 7 events in which threshold speed was exceeded. For the times when threshold speed was exceeded, current directions were dominantly to the ENE as directions ranged from 46 to 110°. There were no currents to the SW during times when threshold speed was exceeded. Bottom currents were quiescent in late winter and spring 2004. Moderate sediment transport events occurred in early- and mid-November 2003 during rapid ice formation period and in the summer 2004 likely related to the storm processes. The strongest event, however, occurred in January 2004 in which peak current speed reached ~60 cm/s and the current direction was 88°. The mean and 95th percentile current speeds were 5.6 and 15 cm/s respectively and sediment erosion occurred in 2.2% of the time. Extrapolated bottom currents for 2004-05 showed 9 events in which bottom currents exceeded the threshold condition (Figure 3-4-6). Bottom currents were weak in the fall 2004 and in the spring and summer 2005. Weak erosion events occurred in early November 2004 and late August 2005. However, stronger current events occurred mostly in the winter (December 2004 and January-March 2005). The current directions in these events were dominantly to the ENE. In the strong current event in mid-January 2005, the maximum bottom currents were eastward and reached 76 cm/s which represents the strongest bottom currents ever measured on the Beaufort outer shelf and upper slope. The mean and 95th percentile current speeds were 6.9 and 21 cm/s respectively and sediment erosion occurred in 6.2% of the time. It is noted that the extreme current event of mid-January 2005 not only recorded the strongest bottom currents of all the mooring data assessed, the event under ice covered conditions also lasted 9.7 days which accounted for ~44% of the total hours of threshold exceedance in 2004-05 at CA04. Similar predominance of this mid-winter event was also observed for the upper slope site CA13 on the eastern Beaufort Shelf (see description below). The magnitude and direction of extrapolated bottom currents for 2005-06 presented in Figure 3-4-7 indicate 9 sediment transport

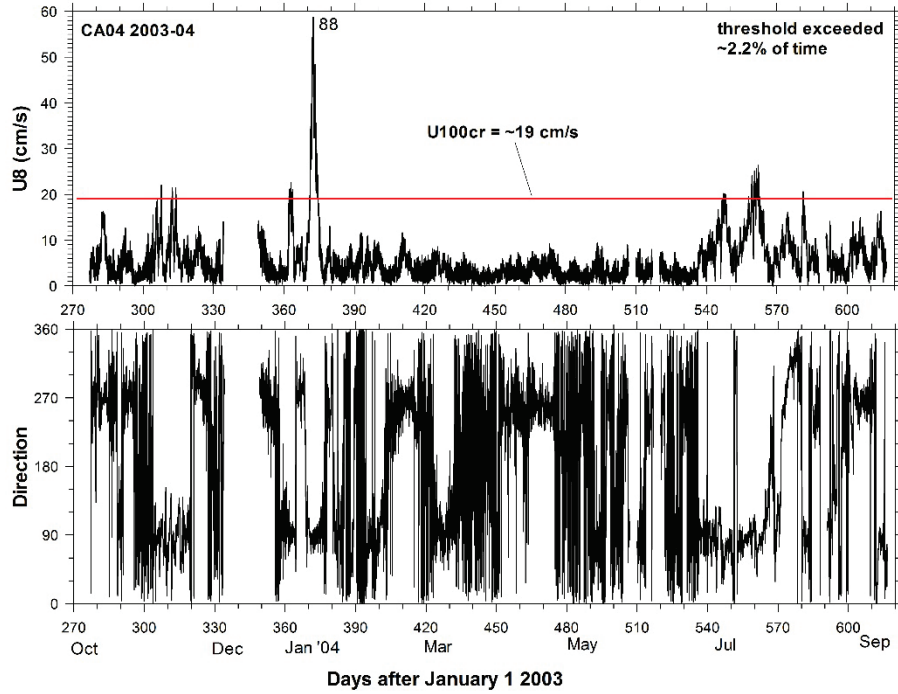


Figure 3-4-5 Magnitude and direction of extrapolated bottom currents for 2003-04 at CA04 site on the upper slope of the eastern Central Beaufort Shelf (ECBS) area. The red line represents the critical current for sediment erosion, U100cr.

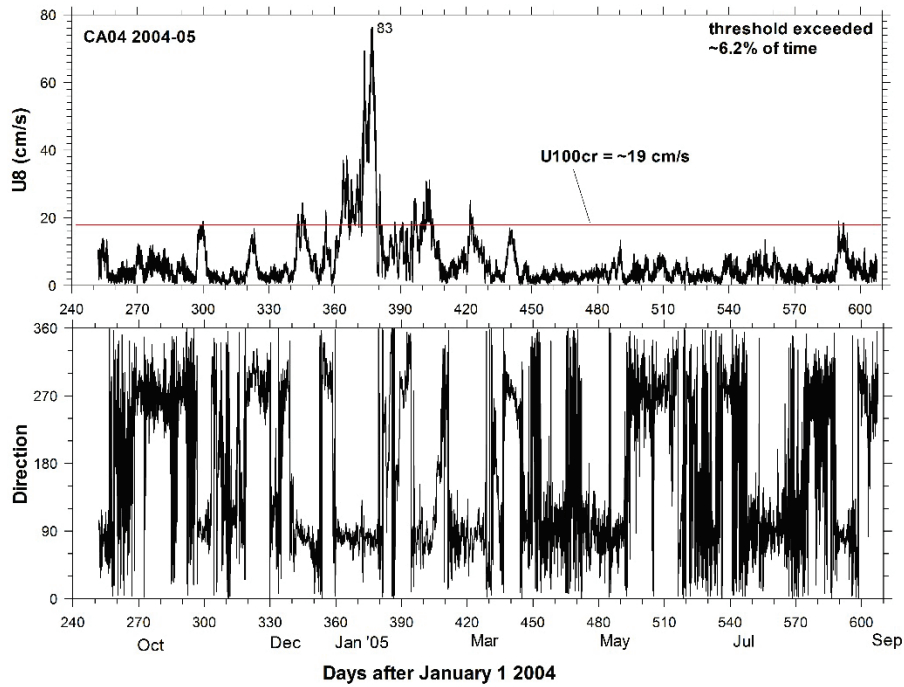


Figure 3-4-6 Magnitude and direction of extrapolated bottom currents for 2004-05 at CA04 site on the upper slope of the eastern Central Beaufort Shelf (ECBS) area. The red line represents the critical current for sediment erosion, U100cr.

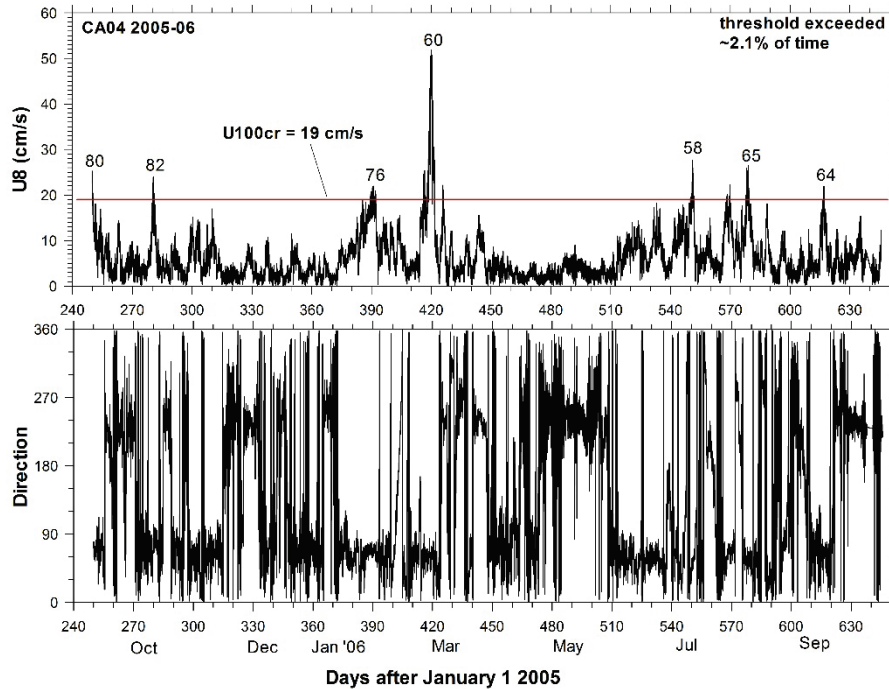


Figure 3-4-7 Magnitude and direction of extrapolated bottom currents for 2005-06 at CA04 site on the upper slope of the eastern Central Beaufort Shelf (ECBS) area. The red line represents the critical current for sediment erosion, U100cr. Numbers mark the direction of currents at the peak of current events.

events in which currents were predominantly to the ENE (89%). Bottom currents were again weak in the spring 2006 and did not cause erosion of sediments. Otherwise sediment erosion events were evenly distributed over the fall, winter and summer seasons for 2005-06. However, the strongest event again occurred in the winter (late February) 2006 in which maximum currents were to the ENE and reached ~52 cm/s. The mean and 95th percentile current speeds were 6.2 and 15 cm/s respectively and sediment erosion occurred in 2.1% of the time.

Site CA07

CA07 is on the middle slope of the eastern central Beaufort Shelf area in 500 m water depth. The two near-by bottom samples suggest silty clay with an average mean grain size of 0.0029 mm. A RCM11 current meter was deployed at 389 m depth to record half-hourly current data at 111 mab from 2003/10/3 to 2004/9/7. For 2004-05, a RCM11 current meter was deployed at 387 m depth to record hourly current data at 113 mab from 2004/9/8 to 2005/6/27 (Table 1). The measured currents at respectively 111 and 113 mab were extrapolated to 8 mab and the magnitude and direction of the extrapolated bottom current data are shown in Figures 3-4-8 and 3-4-9. The statistics of mean, 95th percentile, and maximum current speeds and sediment erosion frequency are listed in Table 5.

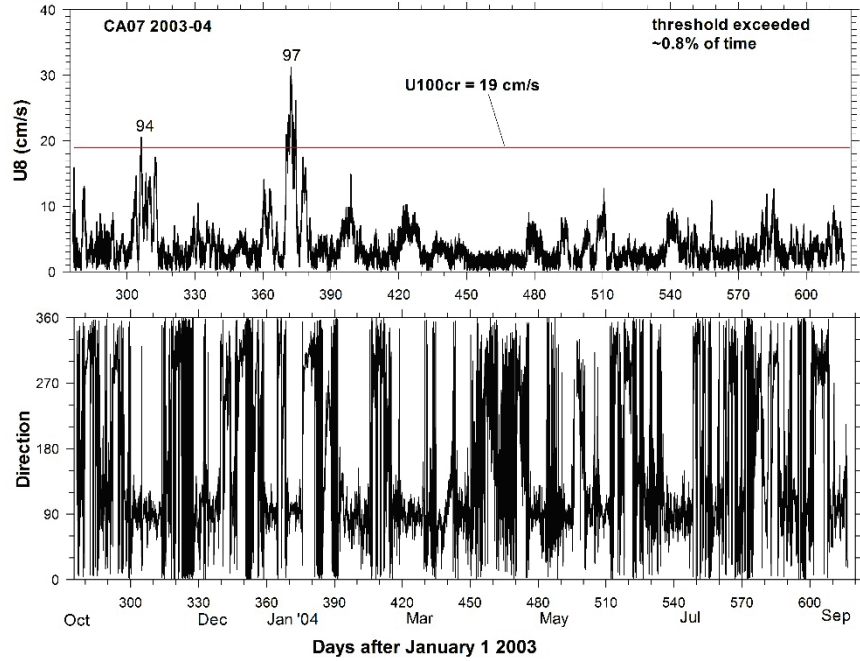


Figure 3-4-8 Magnitude and direction of the extrapolated bottom current data for 2003-04 at CA07 on the slope of the eastern Central Beaufort Shelf (ECBS) area. The red line represents the critical current for sediment erosion, U_{100cr} . Numbers mark the direction of currents at the peak of current events.

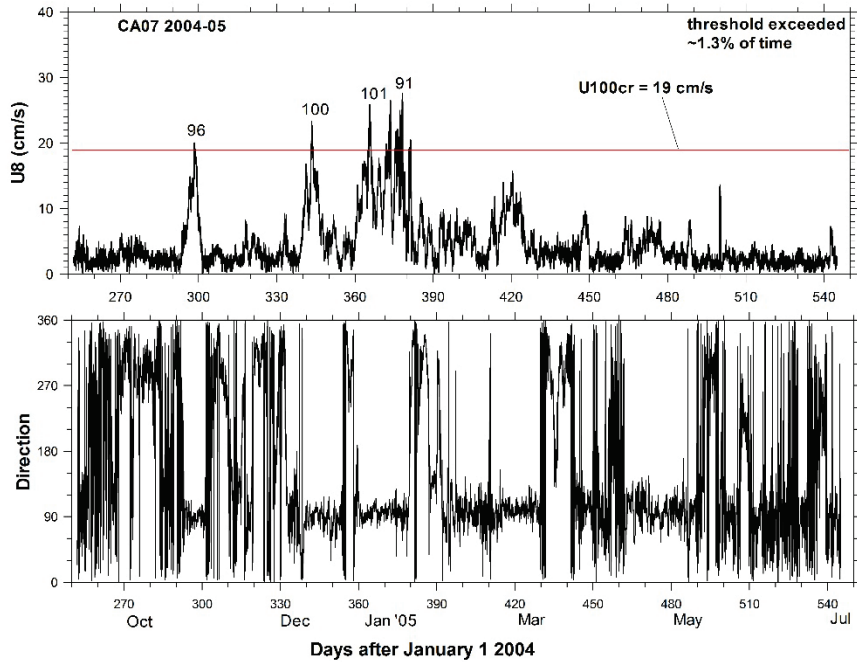


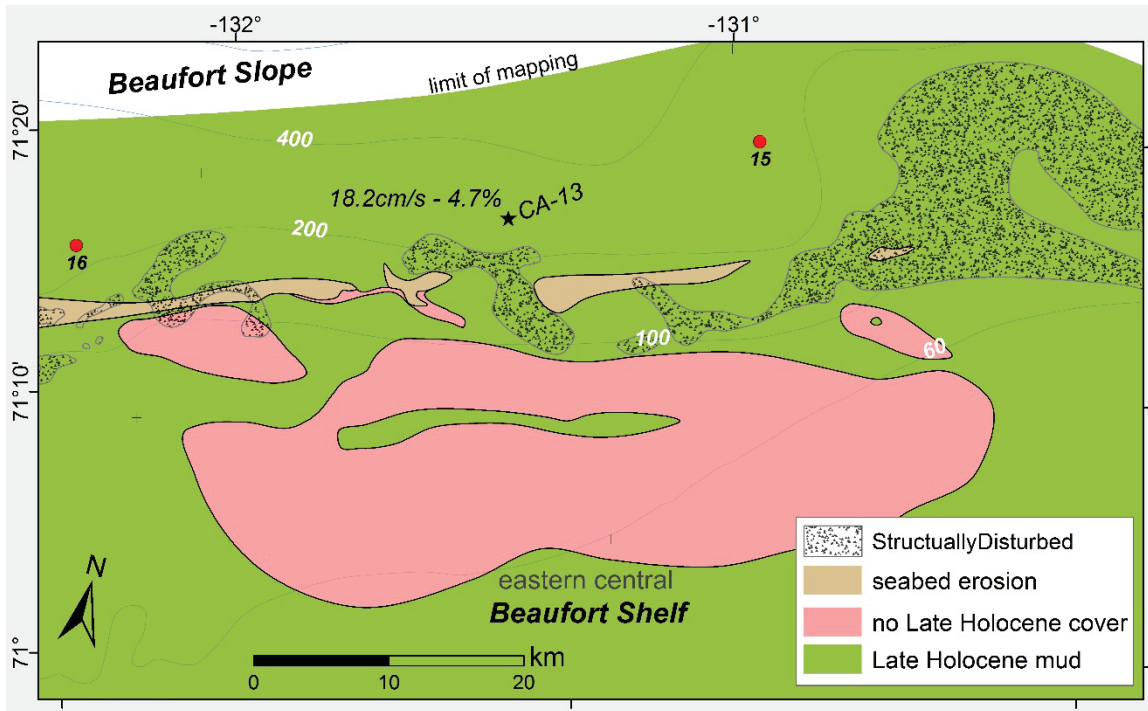
Figure 3-4-9 Magnitude and direction of the extrapolated bottom current data for 2004-05 at CA07 on the slope of the eastern Central Beaufort Shelf (ECBS) area. The red line represents the critical current for sediment erosion, U_{100cr} . Numbers mark the direction of currents at the peak of current events.

The bottom current data for 2003-04 at CA07 (Figure 3-4-8) show that bottom currents were generally less than 19 cm/s and only exceeded the threshold speed in 2 events. Bottom currents reached 21 cm/s and exceeded the threshold for only 2 hours in early November 2003. A stronger event occurred in early January 2004 in which maximum currents reached 31 cm/s and lasted nearly 3 days. Currents were to the east in both events. The mean and 95th percentile current speeds were 3.9 and 10 cm/s respectively and sediments were eroded for merely 0.8% of the time. The maximum bottom currents reached 28 cm/s in 2004-05 (Figure 3-4-9) and exceeded the threshold more frequently (in 6 events) than 2003. Currents were weak and did not cause sediment erosion in the spring and summer. A weak transport event occurred in late October 2004 due to rapid ice formation and several moderate transport events occurred in December 2004 and January 2005 likely due to mid-winter ice fracturing. Currents in these events were again predominantly to the ESE. The extreme mid-January 2005 event observed on the upper slope at CA04 site, also impacted the seabed at the mid-slope site CA07. However, the maximum current speed was <30 cm/s, and the event only lasted ~3 days and did not demonstrate the predominance over other events during the winter months. Both the mean and 95th percentile current speeds were stronger than 2003 and reached 4.5 and 14 cm/s respectively which were correlated with threshold exceedance in 1.3% of the time. Thus the extrapolated bottom current data for 2003-04 and 2004-05 at CA07 suggest that the near-bed currents on the slope were weak in the spring, summer and fall and did not cause sediment transport. Moderate current events mostly occurred in the late fall/early winter due to rapid ice formation and in the winter likely due to mid-winter ice fracturing to cause infrequent sediment erosion and transport that was dominantly to the east and east-southeast.

3.5 Near-bed currents and sediment mobility on the eastern Beaufort Shelf (EBS)

CA13 is on the upper slope of the eastern Beaufort Shelf area in 300 m water depth (Figures 3-5-1). The site is over the late Holocene mud and the two associated bottom samples suggest silty clay with significant sand component. The average mean grain size is 0.0055 mm, the coarsest of all the upper slope sites. A RCM11 current meter was deployed at 217 m depth to record half-hourly current data at 83 mab from 2003/10/9 to 2005/2/10. An ADCP profiler was also deployed at 119 m depth and collected current data averaged for 12 minutes every 45 minutes at 192 mab from 2003/10/9-2005/9/4 (Table 1). Current direction information was not available in the ADCP data. The current data measured respectively at 83 and 192 mab were extrapolated to 8 mab and the magnitude and direction of the extrapolated bottom current data for 2003-04 and 2004-05 are shown in Figures 3-5-2 and 3-5-3 respectively. Statistics of mean, 95th percentile, and maximum current speeds and sediment erosion frequency are listed in Table 6.

The extrapolated bottom currents for 2003-04 at CA13 (Figure 3-5-2) show that bottom currents reached the maximum speed of 51 cm/s and exceeded the threshold in 9 events. Current directions in bursts in which threshold was exceeded were dominantly to the ENE and the ESE



Figures 3-5-1 Map of the mooring site CA13 (star) and associated sediment sample stations (circle; ID in Table 2) superposed on the mapped erosion and non-deposition zone for the eastern Beaufort Shelf (EBS) area. The numbers next to the mooring site name are respectively the 95th percentile speed (cm/s) and sediment erosion frequency (% of time) at the mooring site CA13.

Table 6 Statistics of mean, 95th percentile, maximum bottom current speed and sediment erosion frequency for CA13 site at the eastern Beaufort Shelf (EBS) area. All currents are in cm/s and erosion frequency is in % of the time.				
	Mean (U8)	95 th percentile	Maximum	Erosion Frequency
2003-04	5.8	15.3	51.1	2.5
2004-05	8.5	21.0	67.9	6.9
Average	7.2	18.2	59.5	4.7

(88% of the time) and were to the SW in 8% of the time. Currents were weak in spring and early summer 2004. Weak to moderate transport occurred in the summer and fall. However, the most dominant transport event occurred in winter 2004 and was to the ESE. The mean and 95th percentile current speeds were 5.8 and 15 cm/s respectively and sediment erosion occurred in 2.5% of the time. The bottom currents and sediment erosion for 2004-05 (Figure 3-5-3) were moderately stronger as the maximum bottom currents reached 68 cm/s and caused sediment erosion in 10 events. For September 2004 – February 2005 when current direction data were available, the currents in bursts in which threshold was exceeded were again dominantly to the

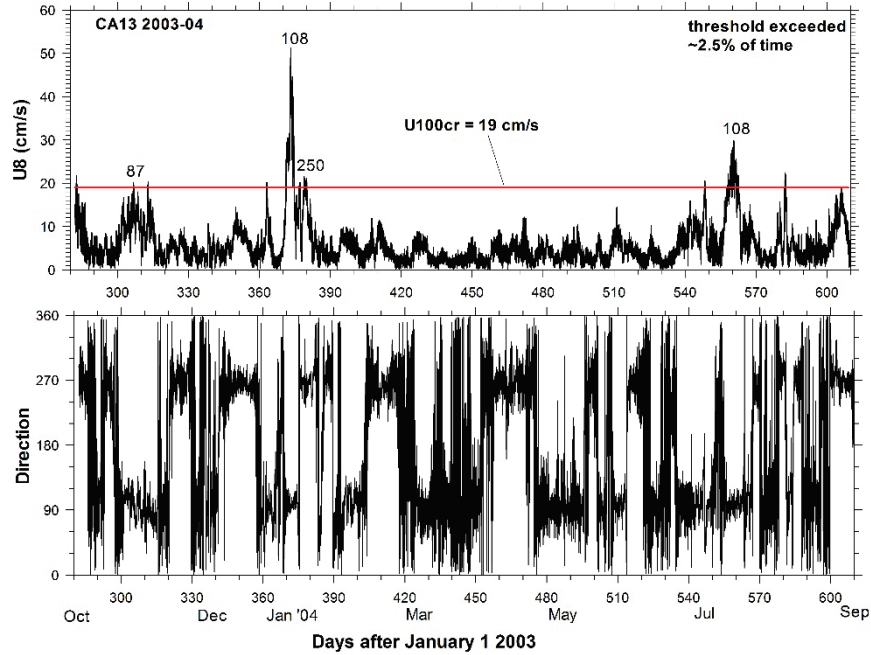


Figure 3-5-2 Magnitude and direction of the extrapolated bottom current data for 2003-04 at CA13 on the slope of the eastern Beaufort Shelf area. The red line represents the critical current for sediment erosion, U100cr. Numbers mark the direction of currents at the peak of current events.

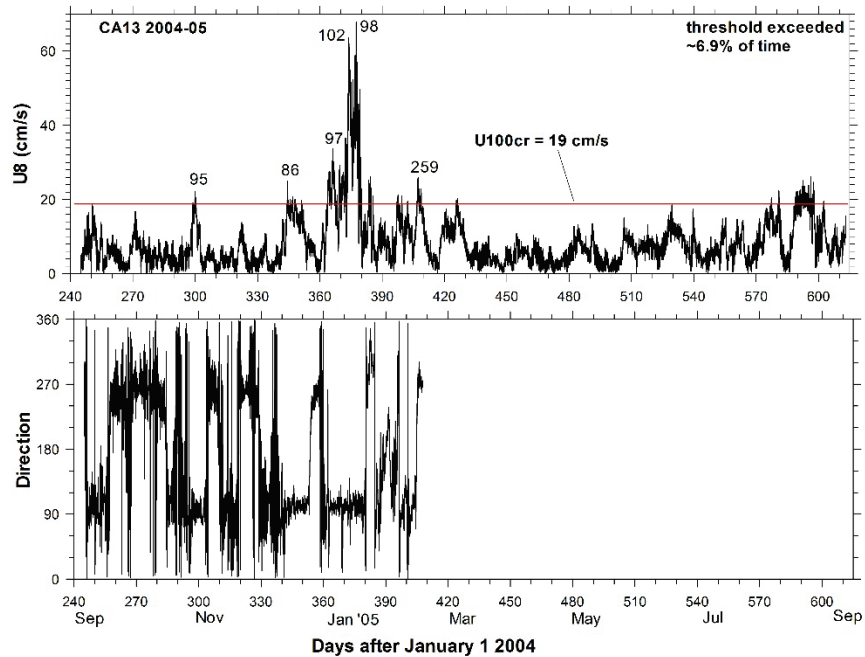


Figure 3-5-3 Magnitude and direction of the extrapolated bottom current data for 2004-05 at CA13 on the slope of the eastern Beaufort Shelf area. The red line represents the critical current for sediment erosion, U100cr. Numbers mark the direction of currents at the peak of current events.

ENE and ESE (88% of the time). Currents in the spring and early summer 2005 were again weak and did not cause sediment transport. Weak transport events occurred in early November 2004 and late summer 2005. Most of the transport events, however, occurred in the winter 2005. Current directions in these events were dominantly to the East and to the ESE. The mean and 95th percentile current speeds were stronger than 2003-04 and were 8.5 and 21 cm/s respectively. Sediment was eroded for 6.9% of the time. Similar to the predominance on bottom current and sediment erosion by the mid-winter event at site CA04 at the ECBS area (see Section 3.4), the dominant effect of this event is extended to the upper slope of the eastern Beaufort Shelf. The 68 cm/s speed at the peak of this event recorded at CA13 represents the second highest bottom currents of all the mooring data assessed on the Beaufort Shelf break and upper slope. The event lasted for ~10.15 days which accounted for 44% of the total time of threshold exceedance in 2004-05 at CA13.

3.6 Discussion of near-bed currents and sediment mobility analyses

3.6.1 Overall characteristics of current intensity and sediment erosion frequency

Previous studies generally noted that hydrodynamic conditions are relatively quiescent on the Beaufort mid- and outer-shelf (Harper and Penland, 1982; Hill et al., 1991). The synthesis of bottom currents and sediment erosion potential of this study demonstrates that currents and sediment mobility on the shelf break and upper slope likely are greater than the mid- and outer shelf. Events with maximum bottom currents of 60-80 cm/s periodically occur and maximum sediment erosion frequency can reach 17% of the time on the Beaufort shelf break and 7% on the upper slope (Tables 3 to 6). Bottom currents and sediment erosion are generally stronger along the shelf break than on the upper slope, particularly at the WBS-MT and WCBS areas (Tables 3 and 4). The yearly 95th percentile current speed ranges 20 – 30 cm/s and sediment erosion frequency ranges 5 – 17% at the shelf break in these areas. The ranges of these parameters on the upper slope decrease to 12 – 16 cm/s and 1 – 3% respectively. The current intensity and sediment erosion potential, however, become nearly equal at the ECBS area as the average 95th percentile current speed was ~17 cm/s and sediment erosion frequency was ~3.5% at both the shelf break site SIC2 and the upper slope site CA04 (Table 5).

The maximum current data in Tables 3 to 6 indicates that the maximum bottom currents at the shelf break are stronger than or equal to that on the upper slope in the WBS-MT and WCBS areas. The relationship, however, is reversed for the ECBS area and likely also for the EBS area. The maximum bottom currents on the upper slope in these areas were much stronger than that at the shelf break, influenced by the extremely strong bottom currents of 70-80 cm/s observed in 2004-05 at these upper slope sites (Tables 5 and 6). Although the strongest bottom currents were observed on the upper slope, 76 cm/s at CA04 and 68 cm/s at CA13, sediment erosion frequency on these upper slope sites was much lower than the shelf break sites in the WBS-MT and WCBS

areas: 2 – 7% vs 5 – 17% of the time. This is attributed to the differences in the occurrence frequency of strong bottom current events for these settings. For instance the number of events with current speeds exceeding 40 cm/s in each year was ~five at BR-2 (Figures 3-2-2 and 3-2-3) and BR-B (Figures 3-3-2 to 3-3-5) while the frequency of such events was roughly once a year at the upper slope sites CA04 (Figures 3-4-5 to 3-4-7) and CA13 (Figures 3-5-2 and 3-5-3).

3.6.2 Seasonality of bottom currents and isobaths control of current direction

The examination of the bottom current data observed at all shelf-break sites (Figures 3-2-2, 3-2-3, 3-3-2 to 3-3-5, 3-4-2 to 3-4-4) demonstrates some common seasonal variations of bottom current intensity and the dependence of the current direction on the orientation of local bathymetry. The overall magnitude and frequency of strong current events tend to be the weakest in the spring, increase moderately in the summer and are the strongest in the fall and winter. In comparison with the upper slope sites (discussed below), the intensity and frequency of strong currents during summer and fall storms on the Beaufort Shelf break are equal to or greater than those during the ice-covered winter months, particularly so at the shallower shelf break site SIC2 (Figures 3-4-2 to 3-4-4) on the eastern central Beaufort Shelf.

The direction of currents at the peak of strong current events is strongly controlled by the local bathymetry and is roughly parallel to the local isobaths. The strongest currents at BR-2 were predominantly to the north and to the SSW, approximately parallel to the north-south oriented local bathymetry in the Mackenzie Trough (Figures 3-2-1 to 3-2-3). The strongest currents at BR-B were to the NE and to the ENE as again conforming to the WSW – ENE orientation of the bathymetric contours (Figures 3-3-1 to 3-3-5). The local isobaths are nearly east-west oriented at SIC2 site. Therefore the strongest currents were predominantly to the east and to the ENE at this shelf-break site on the eastern central Beaufort Shelf (Figures 3-4-1 to 3-4-4).

In contrast to the shelf-break sites, the bottom current data observed at all upper-slope sites (Figure 3-2-4, Figure 3-3-6, Figures 3-4-5 to 3-4-7 and Figures 3-5-2 and 3-5-3) demonstrate that currents were generally the weakest in the spring season, weak to moderate in the summer and fall seasons, and most energetic in the early winter during rapid ice formation and in the ice-covered winter months. The differences in the seasonal patterns for the upper slope and the shelf break would imply that storms of late summer and fall have less effects on the bottom currents in relatively deep waters on the upper slope and that the amplification of the BSJ by cascading cold dense water and formation of eddies associated with mid-winter ice opening (Forest et al. 2015, 2016) was the dominant mechanism for strong bottom currents on the upper slope. The maximum bottom currents during these strong current events in the winter months can reach 50-80 cm/s and the duration of these events range from 2 to 10 days. The direction of the peak currents on the upper slope is also strongly influenced by the orientation of the local isobaths. The direction of the peak currents at AS84 was to the NW and the north due to the north-south

orientation of the Mackenzie Trough. The peak currents were to the NNE at IMP85B as isobaths are oriented SW to NE and to the ENE at CA04 where the isobaths are oriented WSW to ENE. At CA13 on the eastern Beaufort shelf, the directions of the strongest currents were to the east, again conforming to an east-west orientation of the local isobaths.

3.6.3 Inter-annual variabilities

The time series data of near-bed currents and estimated erosion potential were generally for 2 – 4 years. Significantly longer time series data would be needed for adequate characterization of the inter-annual variability. Nevertheless, near-bed currents and estimated sediment erosion frequency on the Beaufort shelf break and upper slope demonstrate strong inter-annual variabilities at all geographic areas. At BR-2, the 95th percentile current speed was 19 cm/s and sediment erosion occurred for 5.3% of the time for 2011-2012 (Table 3). However, in the following year the 95th percentile current was 26 cm/s and sediment erosion occurred for 16% of the time. At BR-B site on the western central Beaufort Shelf, the annual 95th percentile current speeds range from 20 to 30 cm/s and sediment erosion frequency varied from 7 to 17% of the time over the 2009-2013 period (Table 4). The maximum bottom currents also vary significantly from year to year. For instance, the maximum bottom currents ranged from 52 to 76 cm/s for the period of 2003-2006 at CA04 (Table 5) on the upper slope of the eastern Central Beaufort Shelf.

Although overall seasonal patterns of bottom current intensity are demonstrated by the multiple year data (discussed in the previous section), the inter-annual changes of the seasonal patterns can be quite strong. The bottom currents in the spring of 2009-10 at BR-B were the weakest that year and rarely exceeded 19 cm/s (Figure 3-3-2). The currents in the spring of 2010-11, however, reached nearly 40 cm/s and the frequency of strong current events was as high as other seasons (Figure 3-3-3). Bottom currents were strongest (> 50 cm/s) and occurred frequently in the ice-covered winter months (December to March) in 2009-10 and 2010-11 at BR-B. In contrast, bottom currents in the winter months of 2011-12 barely reached 30 cm/s and sediment erosion frequency was thus lower than the summer and fall seasons (Figure 3-3-4). Similar inter-annual changes in the seasonal patterns of bottom currents are also observed at other shelf break sites (e.g. Figures 3-4-2, 3-4-3, 3-4-4 for SIC2 site).

4. Oceanographic processes and distribution of the erosion/non-deposition zone

4.1 Characteristics and distribution of the erosion/non-depositional zone

The surficial geological zones on the map presented in Figure 1 outline the mud deposition (green), the erosion zone (brown), and the non-deposition zone (red). All involve Holocene age sediments radiocarbon dated in cores located at or correlated to the shelf break, both at the seabed and to at least several metres below the sediment surface (King et al. 2017). The Holocene mud (green) is a continuous blanket of 0.5 – 15 m thickness mapped both on the shelf

and upper slope flanks of the erosion and non-deposition zones. The mud deposit is acoustically stratified on the slope where it covers a de-glacial blanket with similar character. The Holocene mud layer thins from locally over 10 m to a few metres at 600 m water depth and beyond. It should be noted that the extent of the Holocene mud distribution in the map figures is constrained by the mapping limit and does not imply that these are the boundaries of this unit on the shelf and on the upper slope; it continues both landward and seaward. The erosion zone (brown) is a narrow belt situated along the shelf break ranging from 0.2 – 15 km in width, generally narrowing eastward and extends ~300 km along the shelf break and uppermost slope in water depths from 70 – 300 m. It is a very narrow belt on the western Mackenzie Trough flank but widest on the outer, eastern flank. It is likely a continuous erosion belt, but not demonstrable where it was interrupted by a large mass failure scarp (Fig. 1) which displaced these sediments far down the slope (Cameron et al. 2019). On both flanks of Kugmallit Canyon the erosion is enhanced (Fig. 3-4-1), and extends to greater water depth, apparently affected by the canyon topography, despite mud deposition in the thalweg. Erosion depth is typically 5 – 20 m, diminishing eastward to a few metres or less before it is entirely unregistered near the mouth of Amundsen Gulf. As stated in the methods section, the non-deposition zone (red) marks the pinchout of the shelf-situated Holocene blanket. The non-deposition zone is recognized in narrow and broad areas from the western to eastern shelf extending over 200 km and varies in width from 0.5 to almost 10 km. Its “zero-edge” is typically convoluted in map view, reflecting the spatial variability of conditions suitable for net deposition. This zone is interpreted as one of mud bypass maintained by the currents responsible for the erosion zone. In theory, the non-deposition zone should be present both landward and seaward of the erosion zone. However, the mapping constraints together with the structural disturbance did not allow the mapping of this unit seaward of the erosion zone. The maximum width of the combined erosion and non-deposition zones is ~15 km on the eastern flank of the Mackenzie Trough and ~18 km on the central Beaufort Shelf. The cause of the seabed erosion must be able to account for many metres of exhumation in the long term; the outer Mackenzie Trough locality experienced over 20 m erosion of sediments demonstrated to post-date the erosion associated with a lower sea level.

4.2 Correlation of erosion/non-depositional zones with oceanographic processes

In a DFO and NRCan collaborative study, a 3-D circulation model was applied in the Beaufort Sea towards demonstrating the pattern of the BSJ surges and its correlation with the mapped erosion/non-deposition zones (Ding and Wu, 2016). The model used is TOPAZ4, the latest version of TOPAZ, a coupled ocean-sea ice data assimilation system for the North Atlantic Ocean and Arctic (Sakov et al., 2012). The model outputs 3-D, daily mean fields of temperature, salinity, velocity and other ocean and ice parameters at 12.5 km resolution. The spatial patterns of the modelled currents at the core of the amplified BSJ for selected events were compared with the distribution of the mapped erosion and non-deposition zones to determine their correlation. The pattern and location of the modelled BSJ matches the mapped 300 km long erosion and non-

deposition belt suggesting a causal relationship (King et al. 2017). The cross- and along-shelf variations of the intensity of near-bed currents and sediment erosion derived in this study are compared with the mapped spatial patterns of the erosion/non-deposition zones to further demonstrate the correlation between mapped erosion/non-depositional zones and present oceanographic processes on the Beaufort shelf break and upper slope.

If the outer shelf site I is translated ~40 km to the southwest roughly parallel with the local isobaths (Figure 3-3-1), Sites I, BR-B, IMP85B, and BR-A1 form an approximate cross-slope transect at the WCBS area. The 95th percentile speed and sediment erosion frequency were averaged for durations ranging 1 - 4 years for these four sites (Table 4). The averaged values are plotted as a function of distance away from the shelf break site BR-B in Figure 4-1a. Currents and sediment erosion were the strongest along the shelf-break at the BR-B site where the averaged 95th percentile current speed was 25 cm/s and the sediment erosion frequency reached 12.4% of the time. At the upper-slope site IMP85B, the 95th percentile current speed decreased substantially to 16 cm/s and sediment erosion frequency also dropped to only 3% of the time. These values were further reduced respectively to 13 cm/s and 1.3% of the time at the slope site BR-A1 (in 660 m water depth). Shoreward from the shelf break, extrapolated bottom currents data at the outer-shelf site I show that the 95th percentile current speed was ~16 cm/s and sediment was eroded in 2% of the time, illustrating that current intensity and sediment erosion potential decrease significantly from the shelf-break (BR-B) to the outer shelf as well. The bottom current intensity and sediment erosion data over the four sites along the cross-slope transect at the WCBS area therefore suggest that the BSJ current surges were the strongest along the Beaufort Shelf break (BR-B site) and decrease significantly both seaward on the upper slope (IMP85B site) and landward on the outer shelf (Site I). Site BR-A1 and Site I likely represent respectively the seaward and landward limits of the impact zone of the amplified BSJ. The width of the zone over which the BSJ surges effectively impact the seabed is estimated as ~20 km at the WCBS area. Mooring sites SIC2, CA04, and CA07 comprise another cross-slope transect at the ECBS area (Table 5 and Figure 3-4-1). Similar variation patterns of current and erosion magnitudes are also found along this across-slope transect at the eastern Central Beaufort Shelf (ECBS) area (Table 5 and Figure 3-4-1). Site I could again represent the outer shelf site of this transect by extrapolating it northeastward to the landward end of the transect. Cross-slope variations of the mean 95th percentile speed and sediment erosion frequency averaged for durations over 2 - 3 years are shown in Figure 4-1b. Along this transect at the ECBS area, bottom currents and sediment erosion were again the strongest at the shelf-break site SIC2 where 95th percentile speed and sediment erosion frequency were 17.5 cm/s and 4% respectively. Current intensity and sediment erosion decreased slightly at the upper slope site CA04 and decreased substantially at the slope site CA07 where 95th percentile speed was 12 cm/s and sediment erosion frequency was ~2%. Landward from the shelf break at the outer-shelf site I, these values also decreased to <16 cm/s and ~2% respectively. These variations suggest that the impact zone of the BSJ surges is 20 – 25 km wide for the ECBS area. Since the maximum width of the

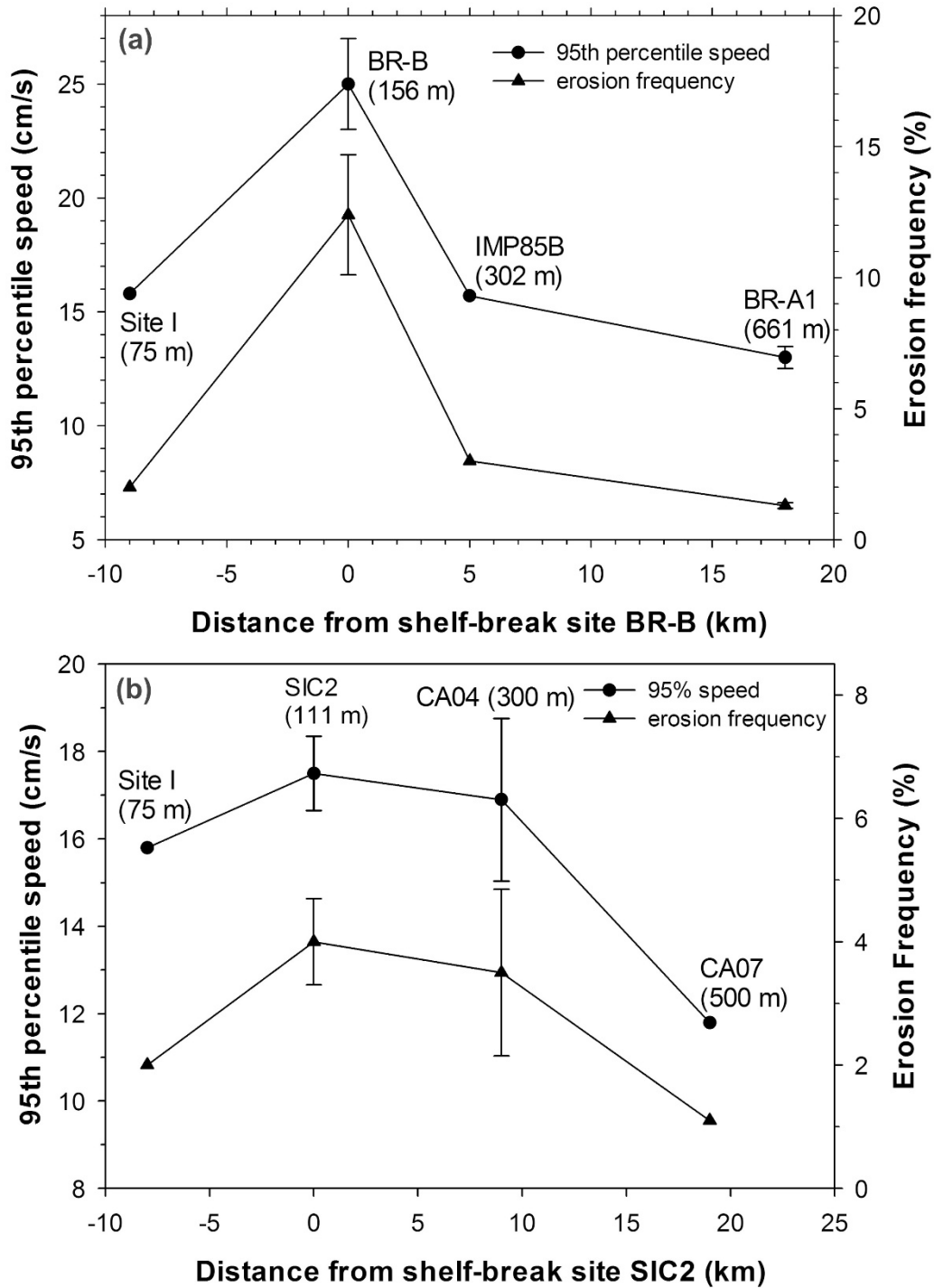


Figure 4-1 Cross-slope variations of the averaged 95th percentile current speed and sediment erosion frequency for transects at (a) WCBS area and (b) ECBS area (averaged over 2011-13 for SIC2). Water depth for each site is shown in parentheses below or next to the site name. Standard errors are shown for sites where yearly means are available for 3 or more years.

combined erosion and non-deposition zones is estimated to be 15 – 18 km, the estimated widths of the BSJ impact zone based on bottom currents and sediment erosion data are in qualitative agreement with the cross-slope scale of the mapped erosion/non-depositional zone.

BR-2, BR-B and SIC2 sites together represent a west to east transect along the shelf break (Figure 1; Tables 3 to 5). The averaged 95th percentile speed and sediment erosion frequency along this along-slope transect over the Beaufort shelf break are shown in Figure 4-2a. The 95th percentile speed and sediment erosion frequency at BR-2 in the WBS-MT area were respectively ~23 cm/s and ~11%. These values decreased slightly to ~22 cm/s and ~9% respectively at BR-B site on the western central Beaufort Shelf and were further reduced to ~18 cm/s and 4% at SIC2 on the eastern central Beaufort shelf. This eastward trend of decreasing bottom current intensity and sediment erosion frequency along the shelf break corroborates the eastward diminishing widths and erosion magnitude of the combined erosion and non-deposition zones described in Section 4.1.

Sites AS84/SS-4b, IMP85B, CA04 and CA13 collectively represent an along-slope transect over the Beaufort upper slope (Figure 1; Tables 3 to 6). The along-slope variations of 95th percentile speed and sediment erosion frequency for these sites are shown in Figure 4-2b. In contrast to the shelf break, 95th percentile speed and sediment erosion frequency data on the upper slope seems to demonstrate a trend of increasing current intensity and sediment erosion frequency from the west to the east. The values of 95th percentile speed steadily increased from ~13 cm/s to ~18 cm/s while that of sediment erosion frequency increased from ~2% to ~5%. However, this along-slope trend for the upper slope setting should be considered tentative given the uncertainty caused by the differences in years and duration of mooring data for the four upper slope sites (see Table 1).

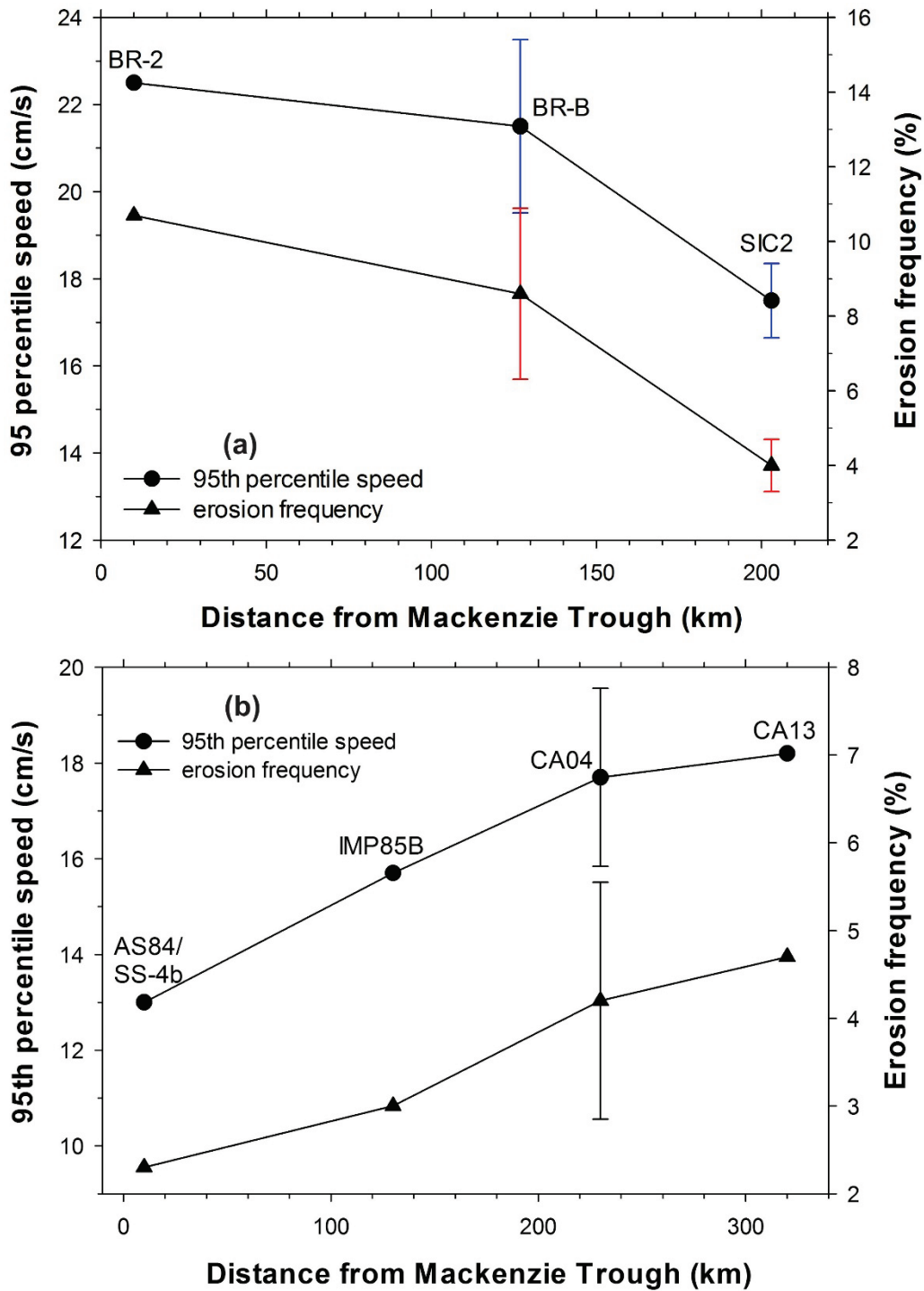


Figure 4-2 Along-slope variation of averaged 95th percentile current speed and sediment erosion frequency (a) over the shelf break (averaged over 2011-13) and (b) over the upper slope (averaged over 2003-05 for CA04 and CA13). Standard errors are shown for sites where yearly means are available for 3 or more years.

5. Summary

Reviews of other studies indicate that present day sediments delivered to the Canadian sector of the Beaufort Sea are predominantly supplied by the Mackenzie River. The river delivers ~125 Mt per year of mainly fine grained sediments. Approximately 50 Mt of this are deposited in the delta, ~60 Mt are deposited on the shelf and ~15 Mt are exported beyond the shelf edge to the continental slope. The sediments discharged from the river move across the shelf to the shelf edge and upper slope via cycles of deposition, resuspension and transport that are mainly controlled by the extensive open water, the dispersal and transport by the turbid Mackenzie River plume, and the intense resuspension and transport by strong waves and wind-driven currents during storms. During the open-water season, high waves and wind-driven currents during storms result in widespread sediment resuspension and transport on the shoreface and inner shelf. Recent observations on the outer shelf suggest that resuspension of fine sediments and their advection to the shelf edge should be expected during downwelling-favorable wind conditions. Once sediments are resuspended, they will be transported across and along the shelf by wind-driven and downwelling currents through the development of both the bottom and intermediate Nepheloid layers. The conditions required to set the Nepheloid layers in motion, however, are not well understood. More process-oriented studies are needed to resolve the mechanisms underlying the formation and motion of the Nepheloid layers and their interaction with the shelf-break jet on the upper slope.

Hydrodynamics on the Beaufort shelf break and slope are dominated by the Beaufort Shelf-break Jet (BSJ) which is a bathymetrically steered, eastward subsurface flow of the Pacific-origin waters trapped along the shelf break and upper slope. The width of BSJ is 10-15 km and its core lies at 50 – 250 m depths. The mean currents are ~9 cm/s and maximum speeds of the amplified BSJ surges can be >100 cm/s. Analyses and interpretation of current and sediment trap data from oceanographic moorings of several previous studies provide preliminary evidence that the presence and current surges of the BSJ, the generation and meandering of eddies associated with the BSJ, and the generation and descending of cold dense winter water are the dominant processes that cause erosion and transport of sediments on the Beaufort shelf edge and upper slope. Thermohaline convection associated with rapid ice formation and downwelling-favorable storm winds act as the main mechanisms that cause the amplification of the BSJ.

Existing mooring and near-bed current data have been compiled from various sources. Current data from 11 sites, spanning from the Mackenzie Trough, eastward to eastern Beaufort Shelf, were selected and analyzed to characterize the shelf break area where earlier work indicated periodic erosion and where recent seabed mapping has delineated this erosion and demonstrated its development through the Holocene. The selected mooring data were collected from 1984 to 2013 and encompass outer shelf to continental slope settings in water depths of 75 – 660 m. The selected current data were mostly measured at 10s to 100 m above bottom. As bottom currents

are required for proper assessment of near-bed currents and sediment mobility, the empirical power law formulae of Soulsby (1997) was applied to extrapolate current speeds measured in the water column to the near-bed values. The measured and extrapolated near-bed current data, largely at 6 - 10 mab, were analyzed and compared with the threshold for sediment erosion to derive a preliminary regional framework of near-bed currents and sediment mobility on the Beaufort Shelf break and upper slope.

Analyses of measured and extrapolated near-bottom currents and the resulting sediment erosion potential demonstrate that currents and sediment mobility on the shelf break and upper slope likely are greater than the mid- and outer shelf. Events with maximum bottom currents of 60-80 cm/s periodically occur and maximum sediment erosion frequency can reach 17% and 7% of the time on the Beaufort shelf break and upper slope respectively. Bottom currents and sediment erosion are generally stronger along the shelf break than on the upper slope. The yearly 95th percentile current speed ranges 20 – 30 cm/s and sediment erosion occurs 5 – 17% of the time at the shelf break near the Mackenzie Trough and on the western Beaufort Shelf. The values of these parameters on the upper slope decrease to 12 – 16 cm/s and 1 – 3% respectively. The direction of currents at the peak of strong current events is strongly controlled by the local bathymetry and is roughly parallel to the local isobaths. The strongest currents at BR-2 on the eastern flank of the Mackenzie Trough were predominantly to the north and to the SSW, while the strongest currents were dominantly to the NE and to the ENE at BR-B on the central Beaufort shelf break.

Bottom currents and inferred sediment erosion show strong seasonal patterns and inter-annual variabilities. At the shelf break, the overall magnitude and frequency of strong current and sediment erosion events tend to be the weakest in the spring, increase moderately in the summer and are the strongest in the fall and winter. On the upper slope, however, the magnitude and frequency of strong currents and sediment erosion are generally the weakest in the spring, weak to moderate in the summer and fall, and most energetic in the early winter during rapid ice formation and in the ice-covered winter months. The intensity and seasonality of the bottom currents and sediment erosion on the Beaufort shelf break and upper slope can also change significantly on a yearly base. The annual 95th percentile current speeds at the shelf break on the western central Beaufort Shelf are found to change from 20 to 30 cm/s and sediment erosion frequency vary from 7 to 17% of the time over the 2009 - 2013 period.

Observed near-bottom currents and estimated sediment erosion frequency along cross-slope transects demonstrate that currents and sediment erosion are the strongest along the shelf break and decrease both seaward on the upper slope and landward on the outer shelf. The width of the impact zone of the amplified BSJ based on the current and sediment erosion data is 20 – 25 km. These are in qualitative agreement with the 15-18 km widths of the mapped erosion and non-deposition zone. In the along slope direction, current intensity and sediment erosion frequency

are found to decrease from the west to the east over the Beaufort Shelf break. This supports the decreasing trend from the west to the east of the width of the mapped erosion and non-deposition zone. These conformities in the cross- and along-slope spatial patterns between the impact zone of the amplified BSJ and the mapped erosion/non-deposition zones suggest that the presence and amplification of the BSJ is likely the mechanism for the genesis and maintenance of the erosion and non-deposition zones on the shelf break and upper slope in the Beaufort Sea. They must have been active on the long term to accomplish many metres of erosion at some localities.

Acknowledgement

The authors would like to thank the Institute of Ocean Sciences of DFO, ArcticNet and KOPRI for making various mooring and geophysical data available for this study. We acknowledge the following oceanographic mooring programs led by ArcticNet: the Long-term Oceanic Observatories project, partnerships with Imperial Oil Resources Limited and British Petroleum Canada and the Southern and Northeastern Beaufort Sea Marine Observatories (BREA). These mooring programs were conducted from the Canadian research icebreaker CCGS Amundsen with the support of the Amundsen Science program funded by the Canada Foundation for Innovation (CFI) Major Science Initiatives (MSI) Fund. We are also grateful for the internal review of this publication by Gordon Cameron. This publication is a contribution of the Beaufort Sea Geohazards Assessment Activity within the Land and Minerals Sector Public Safety Geoscience Program. The research was funded by the Panel of Energy Research and Development (PERD) of the Federal Government of Canada.

References

- Aagaard, K., 1984. The Beaufort Undercurrent. In: Barnes, P.W., Schell, D.M., Reimnitz, E. (Eds.), *The Alaskan Beaufort Sea: Ecosystems and Environments*. Academic Press, New York, pp. 47–74.
- Blasco, S., Bennett, R., Brent, T., Burton, M., Campbell, P., Carr, E., Covill, R., Dallimore, S., Davies, E., Hughes-Clarke, J., Issler, D., Leonard, L., MacKillop, K., Mazzotti, S., Patton, E., Rogers, G., Shearer, J., White, M., 2013. 2010 State of Knowledge: Beaufort Sea Seabed Geohazards Associated with Offshore Hydrocarbon Development; Geological Survey of Canada, Open File 6989, 340 p. doi:10.4095/29261635-48.
- Cameron, G.D.M. and King, E.L., 2019. Mass-failure complexes on the central Beaufort Slope, offshore Northwest Territories; Geological Survey of Canada, Open File 8356, 40 p. <https://doi.org/10.4095/314644>
- Carmack, E.C. and Macdonald, R.W., 2002. Oceanography of the Canadian Shelf of the Beaufort Sea: A Setting for Marine Life. *Arctic*, 55, SUPP. 1, 29–45.
- Carson, M.A., Jasper, J.N. and Conly, F.M., 1998. Magnitude and sources of sediment input to the Mackenzie Delta, Northwest Territories, 1974-94. *Arctic*, 51, 116-124.
- Coachman, L.K., and Barnes, C.A. 1961. The contribution of Bering Sea water to the Arctic Ocean. *Arctic* 14, 147–161.
- Ding, F., and Wu, Y. 2016. Circulation structures on the Beaufort Shelf and their potential contribution to sediment transport from the shelf to deep basin. Unpublished technical report submitted to Natural Resources of Canada for DFO-NRCan Interdepartmental Agreement AGR-4638.
- Dmitrenko, I., Kirillov, S.A., Forest, A., Gratton, Y., Volkov, D., Williams, W.J., Lukovich, J.V., Belanger, C., Barber, D.G., 2016. Shelfbreak current over the Canadian Beaufort Sea continental slope: Wind-driven events in January 2005. *J. Geophys. Res.*, 121, 2447–2468, doi:10.1002/2015JC011514.
- Dyer, K.R., 1986. *Coastal and Estuarine Sediment Dynamics*. Wiley, Chichester, 342pp.
- Forest, A., M. Sampei, H. Hattori, R. Makabe, H. Sasaki, M. Fukuchi, P. Wassmann, and L. Fortier, 2007. Particulate organic carbon fluxes on the slope of the Mackenzie Shelf (Beaufort Sea): Physical and biological forcing of shelf-basin exchanges, *J. Mar. Syst.*, 68, 39-54, doi:10.1016/j.jmarsys.2006.10.008.
- Forest, A., Sampei, M., Rail, M.E., Gratton, Y. and Fortier, L., 2008. Winter pulses of Pacific-origin water and resuspension events along the Canadian Beaufort slope revealed by a bottom-moored observatory, *Proc. IEEE Oceans 2008*, 10747934, 8 pp., doi:10.1109/OCEANS.2008.5152010.

Forest, A., Osborne, P.D., Fortier, L., Sampei, M., Lowings, M.G., 2015. Physical forcings and intense shelf–slope fluxes of particulate matter in the halocline waters of the Canadian Beaufort Sea during winter. *Cont. Shelf Res.* 101, 1–21.

Forest, A., Osborne, P.D., Curtiss, G. and Lowings, M.G., 2016. Current surges and seabed erosion near the shelf break in the Canadian Beaufort Sea: A response to wind and ice motion stress. *Jour. Mar. Systems*, 160, 1-16.

Giovando, L.F., and Herlinveaux, R.H., 1981. A discussion of factors influencing dispersion of pollutants in the Beaufort Sea. *Pacific Marine Science Report*, 81-4.

Harper, J.R. and Penland, P.S., 1982. Beaufort Sea sediment dynamics. Contract Report by Woodward-Clyde Consultants, Victoria, BC to the Geological Survey of Canada, Dartmouth, NS, 125p.

Hequette, A., Desrosiers, M., Hill, P.R. and Forbes, D.L., 2001. The influence of coastal morphology on shoreface sediment transport under storm-combined flows, Canadian Beaufort Sea. *Jour. Coastal Res.* 17, 507-516.

Hill, P.R. and Nadeau, O.C., 1989. Storm-dominated Sedimentation on the Inner Shelf of the Canadian Beaufort Sea. *J. Sedimentary Petrology*, 59, 455-468.

Hill, P.R., S.M. Blasco, J.R. Harper and D.B. Fissel, 1991. Sedimentation on the Canadian Beaufort Shelf. *Continental Shelf Research, Special Issue for the Canadian Continental Shelf Seabed Symposium*, Halifax, Nova Scotia, 11(8-10), 821-842.

Imperial Oil Resources Ventures Limited (IORVL), 2013. Beaufort Sea Exploration Joint Venture Drilling Program, Project Description submitted to Environmental Impact Screening Committee, 455 p.

King, E.L., Li, M.Z., Wu, Y., Forest, A., Melling, H., Blasco, S., Harrison, T., Dallimore, S., Paull, C. and Cameron, G., 2016. A belt of seabed erosion along the Beaufort Shelf-break governed by Holocene evolution of the Beaufort Sea Jet: geological evidence, current measurements and initial oceanographic modelling. Abstract for ArcticNet Annual Scientific Meeting, 5-9 December, 2016, Winnipeg, Manitoba.

King, E.L., Li, M.Z., Wu, Y., Forest, A., Blasco, S., Harrison, P., Robertson, A., Melling, H., Dallimore, S.R., Paull, C.K., and Cameron, G.D.M., 2017. A belt of seabed erosion along the Beaufort Sea margin, offshore Northwest Territories, governed by Holocene evolution of the Beaufort Shelf-break Jet; geological evidence, current measurements, and initial oceanographic modelling; Geological Survey of Canada, Open File 8198, 1 poster. doi:10.4095/299691

Kulikov, E.A., Carmack, E.C., Macdonald, R.W., 1998. Flow variability at the continental shelf break of the Mackenzie Shelf in the Beaufort Sea. *Journal of Geophysical Research* 103, 725–741.

- Li, M.Z., King, E.L., Schillinger, D., Robertson, A.G., and Wu, Y., 2019. Observation of bottom currents and sediment transport from the 2015–2016 year-long deployment of a seabed lander on the shelf edge of the Beaufort Sea, offshore Northwest Territories; Geological Survey of Canada, Open File 8553, 57 p. <https://doi.org/10.4095/314645>
- Lukovich, J.V. and Barber, D.G., 2006. Atmospheric controls on sea ice motion in the southern Beaufort Sea. *Journal of Geophysical Research. D. Atmosphere*, 111 (D18), D18103.
- Macdonald, R. and Yu, Y., 2005. The Mackenzie Estuary of the Arctic Ocean. *The Handbook of Environmental Chemistry*, vol. 5H, p. 91-121, Estuaries, Springer-Verlag Berlin Heidelberg 2005.
- Macdonald, R.W., Solomon, S.M., Cranston, R.E., Welch, H.E., Yunker, M.B., Gobeil, C., 1998. A sediment and organic carbon budget for the Canadian Beaufort shelf. *Mar. Geol.* 144 (4), 255–273.
- MacNeill, M.R. and Garrett, J.F., 1975. Open water surface currents. *Beaufort Sea Technical Report 17*, 113.
- Melling, H., 1993. The formation of a haline shelf front in wintertime in an ice-covered arctic sea. *Continental Shelf Research*, 13, 1123–1147.
- Nikolopoulos, A., Pickart, R.S., Fratantoni, P.S., Shimada, K., Torres, D.J., Jones, E.P., 2009. The western Arctic boundary current at 152 W: Structure, variability, and transport. *Deep Sea Res. Part II*, 56, 1164–1181.
- O'Brien, M.C., Macdonald, R.W., Melling, H., and Iseki, K., 2006. Particle fluxes and geochemistry on the Canadian Beaufort Shelf: Implications for sediment transport and deposition. *Continental Shelf Research*, 26, 41-81.
- O'Brien, M.C., Melling, H., Pedersen, T.F., Macdonald, R.W., 2011. The role of eddies and energetic ocean phenomena in the transport of sediment from shelf to basin in the Arctic. *J. Geophys. Res.*, 116, C08001, <http://dx.doi.org/10.1029/2010JC006890>.
- Osborne, P.D. and Forest, A., 2016. Sediment Dynamics from Coast to Slope - Southern Canadian Beaufort Sea. *Journal of Coastal Research, Special Issue No. 75*, 537-541.
- Paull, C.K., Dallimore, S.R., Caress, D.W., Gwiazda, R., Melling, H., Riedel, M., Jin, Y.K., Hong, J.K., Kim, Y.G., Graves, D. and Sherman, A., 2015a. Active mud volcanoes on the continental slope of the Canadian Beaufort Sea. *Geochemistry, Geophysics, Geosystems*, 16, pp. 3160-3181.
- Paull, C. K., Dallimore, S., Caress, D. W., Gwiazda, R., Lundsten, E. M., Anderson, K., Riedel, M., and Melling, H. 2015b. Slope edge deformation and permafrost dynamics along the arctic shelf edge, Beaufort Sea, Canada. *American Geophysical Union, Fall Meeting 2015*, abstract id. OS22B-07.

- Pelletier, B.R., 1975. Sediment dispersal in the southern Beaufort Sea. Department of the Environment, Victoria, BC, Beaufort Sea Project, Technical Report No. 25a, 80 p.
- Pickart, R. S., 2004. Shelfbreak circulation in the Alaskan Beaufort Sea: Mean structure and variability, *J. Geophys. Res.*, 109, C04024, doi:10.1029/2003JC001912.
- Pickart, R.S., T.J. Weingartner, L.J. Pratt, S. Zimmermann and D. J. Torres, 2005. Flow of winter-transformed Pacific water into the Western Arctic, *Deep Sea Research Part II: Topical Studies in Oceanography*, vol. 52, pp. 3175-3198.
- Saint-Ange, F., Kuus, P., Blasco, S., Piper, D.J., Clarke, J.H. and MacKillop, K., 2014. Multiple failure styles related to shallow gas and fluid venting, upper slope Canadian Beaufort Sea, northern Canada. *Marine Geology*, 355, pp.136-149.
- Sakov, P., Counillon, F., Bertino, L., Lisæter, K.A. Oke, P.R. and Korabely, A., 2012. TOPAZ4: an ocean-sea ice data assimilation system for the North Atlantic and Arctic. *Ocean Science* 8, 633-656.
- Soulsby, R.L., 1983. The bottom boundary layer of shelf seas. In: Johns, B. (Ed.), *Physical Oceanography of Coastal and Shelf Seas*. Elsevier Science Publishers, Amsterdam, pp. 189–266.
- Soulsby, R., 1997. *Dynamics of Marine Sands*, 272 pp., Thomas Telford, London.
- Swail, V.R., Cardone, V.J., Ferguson, M., Gummer, D.J., Cox, A.T., 2007. MSC Beaufort Sea Wind and Wave Reanalysis. 10th International Wind and Wave Workshop, Oahu, Hawaii November 11–16, 2007.
- Walker, T. R., J. Grant, P. Cranford, D. G. Lintern, P. Hill, P. Jarvis, J. Barrell, and C. Nozais, 2008. Suspended sediment and erosion dynamics in Kugmallit Bay and Beaufort Sea during ice-free conditions. *J. Mar. Syst.*, 74, 794–809, doi:10.1016/j.jmarsys.2008.01.006.
- Williams, W.J. and Carmack, E.C., 2010. The effect of retreating summer ice on shelf-break exchange in the Arctic Ocean. Abstract and poster presentation, Ocean Sciences Meeting 2010, 22-26 February 2010, Portland, Oregon.
- Woodworth-Lynas, C., Blasco, S, Duff, D., Fowler, J., İşler, E.B., Landva, J., Cumming, E., Caines, A, and Smith, C. 2016. Regional assessment of seabed geohazard conditions, Canadian Beaufort outer shelf and upper slope: Legacy data synthesis: Section 2, Geophysical and geological data compilation, outer shelf and upper slope southern Beaufort Sea: a Handbook of geohazard conditions. Technical Report to Environmental Studies Research Fund Report 208-2. <https://www.esrfunds.org/sites/www.esrfunds.org/files/publications/ESRF208-2-Woodworth-Lynas-Blasco.pdf>